The Influence of Aerosol Hygroscopicity on Clouds and Precipitation over Western Ghats, India

Avishek Ray[1], Moumita Bhowmik[1], Anupam Hazra[1], and Govindan Pandithurai[1]

[1]Indian Institute of Tropical Meteorology

March 14, 2023

Abstract

We examine the role of aerosol hygroscopicity ($\varkappa$) affects clouds and precipitation formation over the Western Ghats (WG) in India using various numerical model simulations (i.e., particle-by-particle based small-scale, high resolution mesoscale model). For the diffusional growth of cloud droplets, the size dependent hygroscopicity is used in $\varkappa$- Köhler equation of direct numerical simulation. The results of the small-scale model reveal that the distribution of cloud drop size varies from the initial mixing state to well mix state due to variation in $\varkappa$. The value of $\varkappa$ is obtained from HTDMA instruments at High Altitude Cloud Physics Laboratory, India. The idealized and real simulations using WRF model with aerosol-aware Thompson microphysics scheme are conducted by changing $\varkappa$ values. Depending on the type of clouds (shallow or deep), different $\varkappa$ values determine the mass, number and precipitation of cloud and rain droplets. Low hygroscopicity (organics) simulates more and smaller drops, as well as uplifts below freezing level, resulting in more ice phase hydrometeors. Organic aerosols have a significant impact on the formation of more snow and graupel hydrometeors. As compared to high $\varkappa$, low hygroscopicity weakens updrafts at the intermediate level and strengthens them at the upper level in the deep cloud region. The intensity of precipitation varies due to low and high $\varkappa$. The findings indicate that aerosol composition has a significant impact on the activation of cloud condensation nuclei. This study suggests that aerosol hygroscopicity is essential in weather prediction models in order to integrate aerosol chemical compositions.

Hosted file

`958225_0_art_file_10782615_rr90mz.docx` available at https://authorea.com/users/594763/articles/629086-the-influence-of-aerosol-hygroscopicity-on-clouds-and-precipitation-over-western-ghats-india

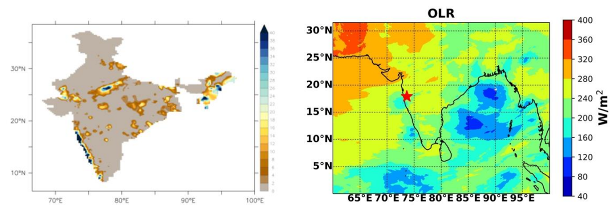
30°N
20°N
10°N
70°E
80°E
90°E
100°E
OLR
30°N
25°N
20°N
15°N
10°N
5°N
65°E 70°E 75°E 80°E 85°E 90°E 95°E
400
360
320
280
240
200
160
120
80
40
W/m^2

Figure 1:

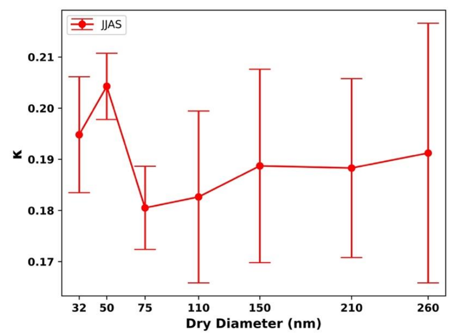
JJAS
0.21
0.20
0.19
0.18
0.17
K
32 50 75 110 150 210 260
Dry Diameter (nm)

Figure 2:

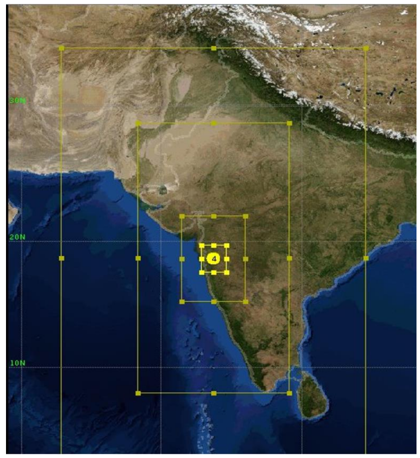

Figure 3:

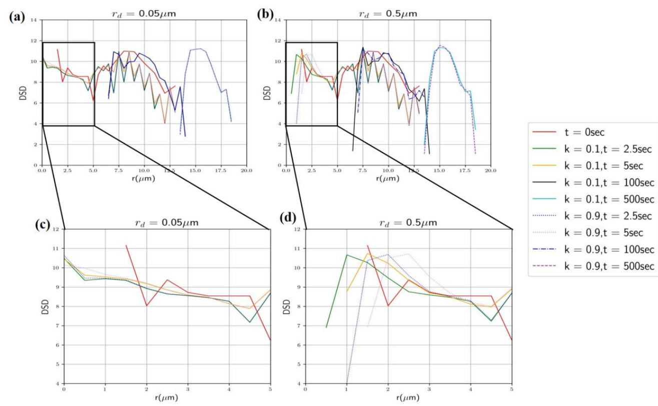
(a)
r_d = 0.05μm
(b)
r_d = 0.5μm
(c)
r_d = 0.05μm
(d)
r_d = 0.5μm
DSD
r(μm)
t = 0sec
k = 0.1,t = 2.5sec
k = 0.1,t = 5sec
k = 0.1,t = 100sec
k = 0.1,t = 500sec
k = 0.9,t = 2.5sec
k = 0.9,t = 5sec
k = 0.9,t = 100sec
k = 0.9,t = 500sec

Figure 4

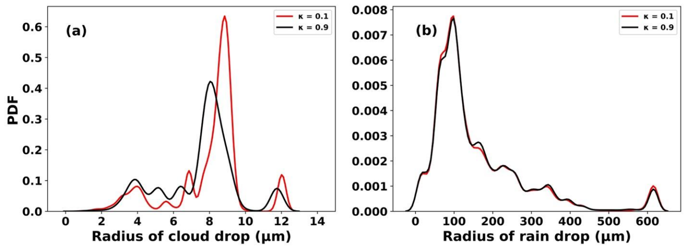

Figure 5:

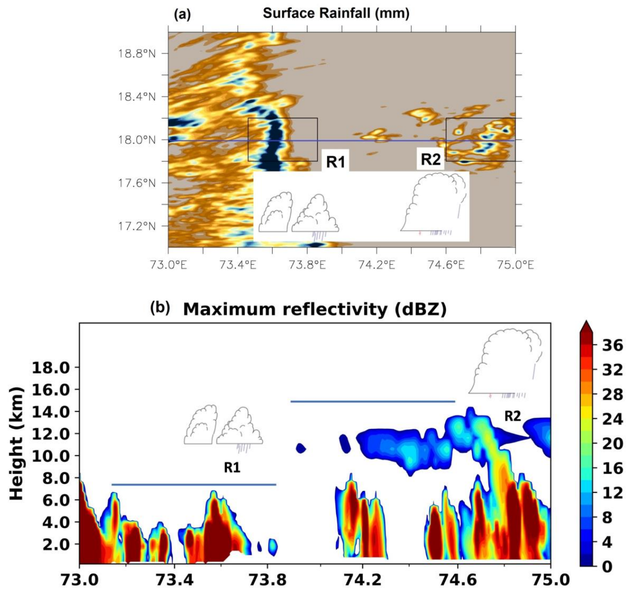
(a)
Surface Rainfall (mm)
18.8°N
18.4°N
18.0°N
17.6°N
17.2°N
73.0°E
73.4°E
73.8°E
74.2°E
74.6°E
75.0°E
R1
R2
(b)
Maximum reflectivity (dBZ)
Height (km)
18.0
16.0
14.0
12.0
10.0
8.0
6.0
4.0
2.0
73.0
73.4
73.8
74.2
74.6
75.0
R1
R2
36
32
28
24
20
16
12
8
4
0

Figure 6

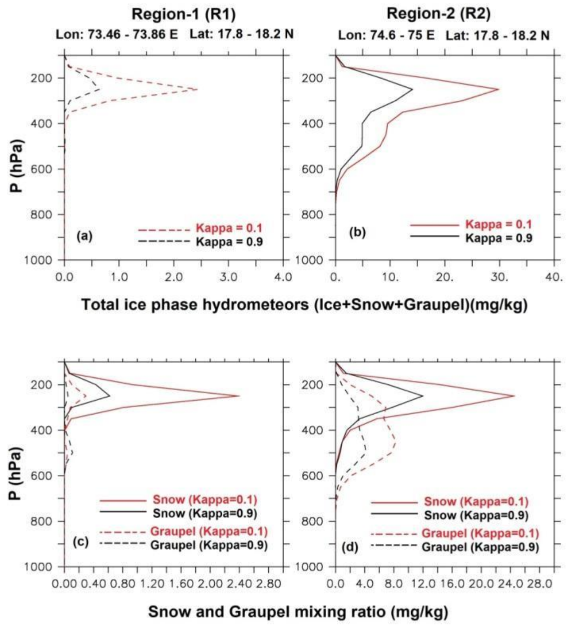

Region-1 (R1)
Lon: 73.46 - 73.86 E Lat: 17.8 - 18.2 N
Region-2 (R2)
Lon: 74.6 - 75 E Lat: 17.8 - 18.2 N
P (hPa)
(a)
Kappa = 0.1
Kappa = 0.9
(b)
Kappa = 0.1
Kappa = 0.9
Total ice phase hydrometeors (Ice+Snow+Graupel)(mg/kg)
(c)
Snow (Kappa=0.1)
Snow (Kappa=0.9)
Graupel (Kappa=0.1)
Graupel (Kappa=0.9)
(d)
Snow (Kappa=0.1)
Snow (Kappa=0.9)
Graupel (Kappa=0.1)
Graupel (Kappa=0.9)
Snow and Graupel mixing ratio (mg/kg)

Figure 7:

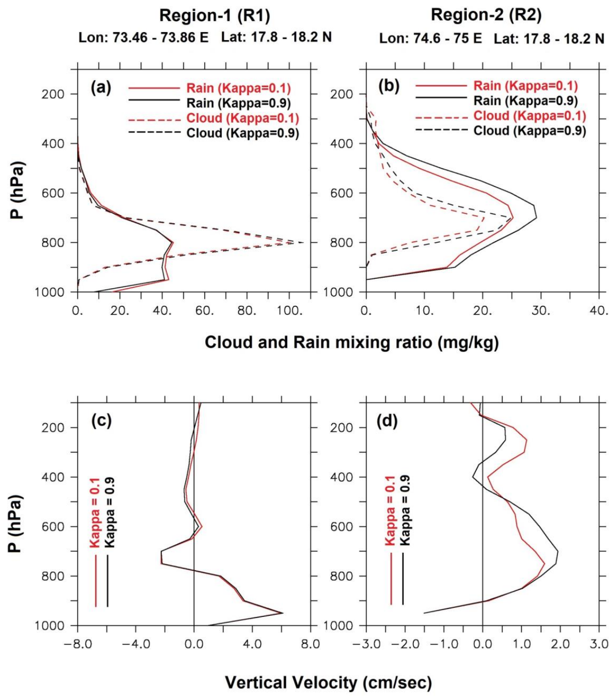

Region-1 (R1)
Lon: 73.46 - 73.86 E Lat: 17.8 - 18.2 N
Region-2 (R2)
Lon: 74.6 - 75 E Lat: 17.8 - 18.2 N
(a)
(b)
Rain (Kappa=0.1)
Rain (Kappa=0.9)
Cloud (Kappa=0.1)
Cloud (Kappa=0.9)
P (hPa)
Cloud and Rain mixing ratio (mg/kg)
(c)
(d)
Kappa = 0.1
Kappa = 0.9
Vertical Velocity (cm/sec)

Figure 8

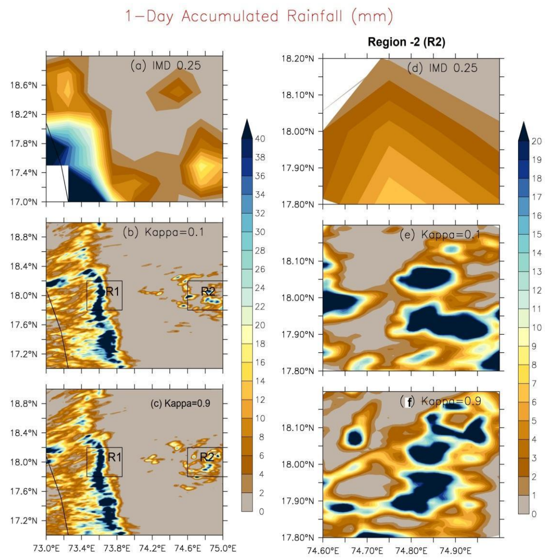
1−Day Accumulated Rainfall (mm)
Region -2 (R2)
(a) IMD 0.25
(b) Kappa=0.1
(c) Kappa=0.9
(d) IMD 0.25
(e) Kappa=0.1
(f) Kappa=0.9
R1
R2
18.6°N
18.2°N
17.8°N
17.4°N
17.0°N
18.8°N
18.4°N
18.0°N
17.6°N
17.2°N
73.0°E
73.4°E
73.8°E
74.2°E
74.6°E
75.0°E
18.20°N
18.10°N
18.00°N
17.90°N
17.80°N
74.60°E
74.70°E
74.80°E
74.90°E

Figure 9:

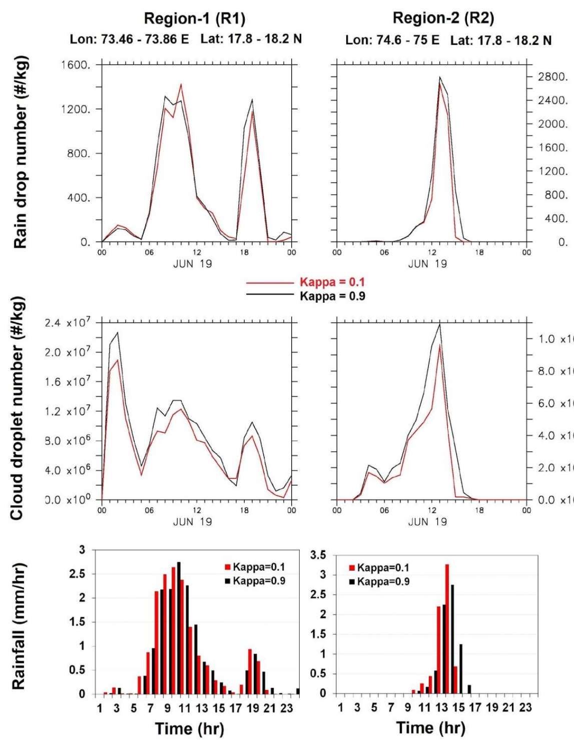
Region-1 (R1)
Lon: 73.46 - 73.86 E Lat: 17.8 - 18.2 N
Region-2 (R2)
Lon: 74.6 - 75 E Lat: 17.8 - 18.2 N
Rain drop number (#/kg)
JUN 19
Kappa = 0.1
Kappa = 0.9
Cloud droplet number (#/kg)
Rainfall (mm/hr)
Kappa=0.1
Kappa=0.9
Time (hr)

Figure 10:

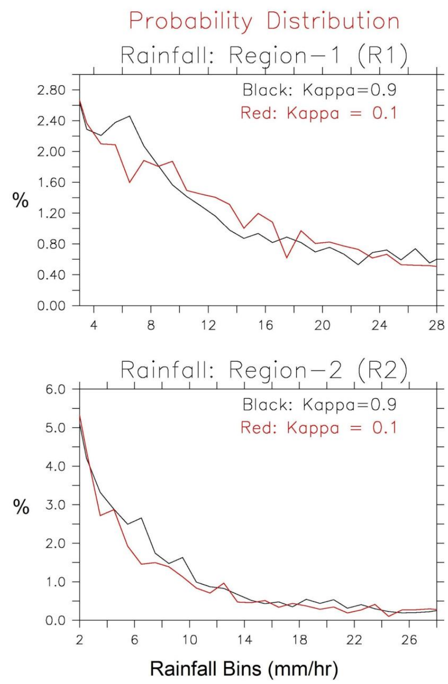
Probability Distribution
Rainfall: Region−1 (R1)
Black: Kappa=0.9
Red: Kappa = 0.1
%
Rainfall: Region−2 (R2)
Black: Kappa=0.9
Red: Kappa = 0.1
%
Rainfall Bins (mm/hr)

Figure 11:

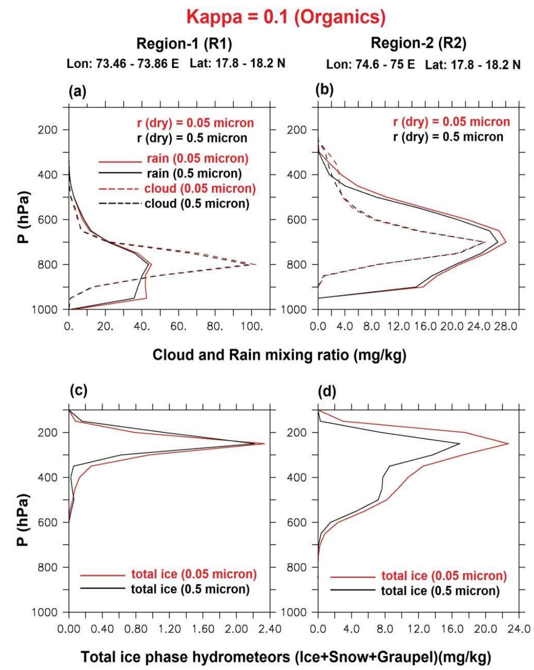

Kappa = 0.1 (Organics)
Region-1 (R1)
Lon: 73.46 - 73.86 E Lat: 17.8 - 18.2 N
Region-2 (R2)
Lon: 74.6 - 75 E Lat: 17.8 - 18.2 N
(a)
(b)
r (dry) = 0.05 micron
r (dry) = 0.5 micron
rain (0.05 micron)
rain (0.5 micron)
cloud (0.05 micron)
cloud (0.5 micron)
P (hPa)
Cloud and Rain mixing ratio (mg/kg)
(c)
(d)
total ice (0.05 micron)
total ice (0.5 micron)
Total ice phase hydrometeors (Ice+Snow+Graupel)(mg/kg)

Figure 12:

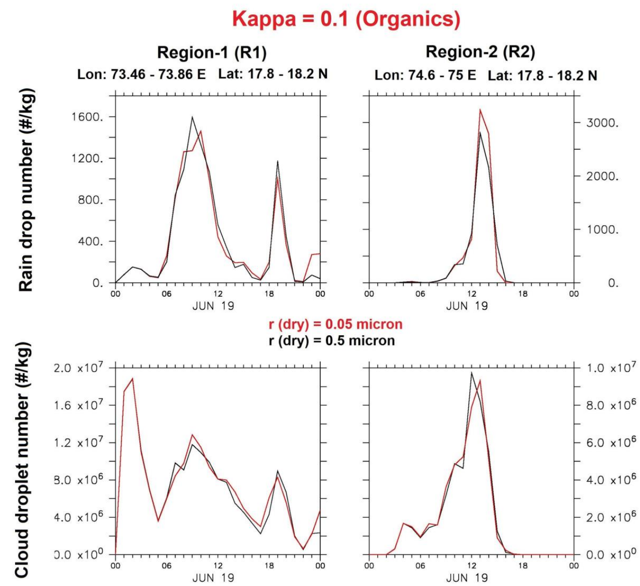
Kappa = 0.1 (Organics)
Region-1 (R1)
Lon: 73.46 - 73.86 E Lat: 17.8 - 18.2 N
Region-2 (R2)
Lon: 74.6 - 75 E Lat: 17.8 - 18.2 N
Rain drop number (#/kg)
Cloud droplet number (#/kg)
JUN 19
r (dry) = 0.05 micron
r (dry) = 0.5 micron

Figure 13:

The Influence of Aerosol Hygroscopicity on Clouds and Precipitation over Western Ghats, India

Avishek Ray[1,2], Moumita Bhowmik[1], Anupam Hazra[1*], and G. Pandithurai[1]

[1]Indian Institute of Tropical Meteorology, Ministry of Earth Sciences, Pune, India.
[2]S. P. Pune University, Pune, India.

Corresponding author: Anupam Hazra (hazra@tropmet.res.in)

Key Points:

- Composition of aerosol particles can impact on the formation of cloud condensates.
- Aerosol hygroscopicity modulates the formation of vertical distribution of hydrometeors.
- Hygroscopicity can influence rainfall intensity and impacts vertical velocity.

Abstract

We examine the role of aerosol hygroscopicity (κ) affects clouds and precipitation formation over the Western Ghats (WG) in India using various numerical model simulations (i.e., particle-by-particle based small-scale, high resolution mesoscale model). For the diffusional growth of cloud droplets, the size dependent hygroscopicity is used in κ- Köhler equation of direct numerical simulation. The results of the small-scale model reveal that the distribution of cloud drop size varies from the initial mixing state to well mix state due to variation in κ. The value of κ is obtained from HTDMA instruments at High Altitude Cloud Physics Laboratory, India. The idealized and real simulations using WRF model with aerosol-aware Thompson microphysics scheme are conducted by changing κ values. Depending on the type of clouds (shallow or deep), different κ values determine the mass, number and precipitation of cloud and rain droplets. Low hygroscopicity (organics) simulates more and smaller drops, as well as uplifts below freezing level, resulting in more ice phase hydrometeors. Organic aerosols have a significant impact on the formation of more snow and graupel hydrometeors. As compare to high κ, low hygroscopicity weakens updrafts at the intermediate level and strengthens them at the upper level in the deep cloud region. The intensity of precipitation varies due to low and high κ. The findings indicate that aerosol composition has a significant impact on the activation of cloud condensation nuclei. This study suggests that aerosol hygroscopicity is essential in weather prediction models in order to integrate aerosol chemical compositions.

Keywords: Hygroscopicity, Numerical model, Cloud and precipitation

Plain Language Summary

Hygroscopicity determines water uptake capacity and hence organics and inorganics are modulating the hygroscopic growth of cloud droplets over Western Ghats, India. The conventional Köhler theory needs to be modified to incorporate the complex chemical composition with the help of aerosol hygroscopicity. We have used κ- Köhler r theory in particle-by-particle based small-scale model and in aerosol-aware Thompson microphysics scheme. The observed hygroscopicity is measured using a Humidified Tandem Differential Mobility Analyzer at High Altitude Cloud Physics Laboratory situated in Mahabaleshwar, Western Ghats. The particle-by-particle based small-scale model results show that size distribution of cloud droplets changes from initial mixing state to well mix state due to changes in κ, which provides a better understanding of droplets activation during initial time period and its effect on the growth of cloud droplets. Subsequently, high resolution WRF simulations with inorganic (high κ) and organic (low κ) aerosols are performed to demonstrate the influence of κ values on the cloud and rain droplets. Organic aerosols have a substantial influence on mixed-phase cloud hydrometeors. The findings show how hygroscopicity affects updrafts and probability distribution of rainfall. These results imply that hygroscopicity will be essential in future model investigations with different aerosol compositions.

1 Introduction

The Indian summer monsoon rainfall (ISMR), defined by the accumulative rainfall throughout June to September (JJAS), characterizes a major heat source in the tropical climate system. Monsoon rainfalls have a significant impact on agriculture and water resource management (Parthasarathy et al. 1994). One important specific feature of seasonal mean monsoon rainfall is the narrow maxima of rainfall, which is oriented coastally along the Western Ghats. Mukherjee et al. (2018) have shown the seasonal deviation of chemically evolved sub-micron aerosol particles (diameter < 1 μm). They have also reported that the isoprene derived Secondary Organic Aerosol (SOA) contributed ~17% to the total Organic Aerosol (OA). Vlasenko et al. (2009) have shown that the oxidation state of the aerosol correlates with the photochemical age of the air, which is important for the SOA mass and can be produced from monoterpene oxidation (Slowik et al. 2010).

Hygroscopicity (kappa or κ) determines the capacity of particles to absorb water under atmospheric circumstances such as temperature and relative humidity. As a result, hygroscopicity refers to the ability of water absorption or adsorption by aerosols as a function of relative humidity. It regulates the size (hygroscopic growth) and refractive index of aerosols, influencing their optical characteristics and hence, prompting visibility and direct radiative forcing (Malm et al. 2005; Cheng et al. 2008). The activation of aerosols to Cloud Condensation Nuclei (CCN) is also strongly connected to hygroscopicity (κ) (Petters and Kreidenweis, 2007; Farmer et al. 2015).

Understanding the hygroscopic properties of aerosols and the processes governing cloud droplet activation is important for numerical weather prediction. Aerosols activation is determined by its size and complex chemical composition, which is crucial for cloud formation processes. The water activity of inorganic aerosols can be calculated by knowing the physio-chemical properties of the solution, which can then be used directly in the Kohler theory for droplet formation. Yet, in a realistic atmosphere, aerosol comprises a large number of organics as well as a mixture of different chemical species, making it more complex. Organics and NH4NO3 are the primary inorganics aerosols influencing hygroscopic growth in North India (Mandariya et al., 2020). Ray et al. (2023) have shown how organics and different inorganic aerosols are modulating the hygroscopic growth across India's Western Ghats region.

The conventional Köhler theory, which describes equilibrium sizes of hygroscopic aerosol particles in humid air, is formulated by taking solubility limitation and curvature effect (Chen, 1994) into account. Since, hygroscopicity is linked to water activity; the thermodynamics of solution determines the aerosols liquid water (Wang et al. 2018). As a result, a better understanding of hygroscopicity is essential in numerical models to better predict the size distribution and consequently radiation under changing humidity conditions (Randall et al. 2007). The increased cross-sectional area of aerosols in high ambient relative humidity conditions is related to the hygroscopic growth of aerosols (Tang and Munkelwitz, 1994).

Highly hygroscopic aerosols may cause precipitation to be delayed by increasing the cloud lifetime. Locally delayed precipitation might energize convective clouds, resulting in heavy rainfall (Rosenfeld et al. 2008). Recently, Kawecki and Steiner, (2018) have shown the role of aerosol composition on precipitation intensity using the Weather and Research Forecasting Model with Chemistry (WRF-Chem). They have calculated the probability distribution of hygroscopicity (κ) for different aerosol chemistry compositions and demonstrated the effect of chemistry on precipitation intensity through hygroscopicity change. The changes in precipitation intensity are basically due to modifications of chemical composition through κ

during mesoscale convective event over Kansas City (Kawecki and Steiner, 2018). Yet, there is no work reported on the role of hygroscopicity (κ) on cloud and precipitation formation over the Indian subcontinent using cloud resolving model (WRF).

While aerosol composition is studied in detail within the atmospheric chemistry community, composition effects are not traditionally included in meteorology models because of limited computing capabilities and the prioritization of efficiently representing microphysical processes (Ghan & Schwartz, 2007; Khain et al. 2015). In many studies (Carrió, Cotton, & Cheng, 2010; Eidhammer et al. 2014; Van der Heever et al. 2006), CCN fields are prescribed using a fixed chemical composition of ammonium sulfate. For the activation of droplets, an atmospheric aerosol particle needs to overcome the Kelvin effect, and determination of water activity of wet particle is crucial.

For the first time, we investigate the sensitivity of the hygroscopicity for convective events over the Western Ghats in India in this manuscript. We have used κ-Köhler theory (Petters and Kreidenweis, 2007, 2008), which simplifies the inclusion of complex chemical composition using aerosol hygroscopicity. To evaluate the growth of aerosols, a humidified tandem differential mobility analyzer (HTDMA) is used, which also determines particle hygroscopicity (Ray et al., 2023). The overall κ of the aerosol is calculated using the growth factor obtained from HTDMA measurements.

In this present endeavor, the cloud droplet size distributions (CDSD) are first estimated theoretically using numerical simulation for two hygroscopicity and dry aerosol sizes to to understand the growth rate processes. Secondly, to answer the question: Does the aerosol hygroscopicity impact rainfall intensity?, 2D idealized and 3D real simulations are performed using Weather Research Forecasting (WRF) model to explore the role of aerosol hygroscopicity on a convective event. To assess the sensitivity of cloud formation and precipitation intensity to κ, we simulate a shallow convective system during monsoon over the Western Ghats (WG) region in India. Several previous studies (Kumar et al. 2014; Konwar et al. 2014; Maheshkumar et al. 2014) have revealed shallow convection dominates the that abundance of rainfall across Western Ghats (WG) regions. We have selected a case of 19 June 2019 for the sensitivity studies of hygroscopicity on a shallow convective event with plenty of rainfall over coastal regions (Fig. 1a). The shallow convection is represented by the higher outgoing long-wave radiation (OLR) from MOSDAC INSAT3D satellite (https://www.mosdac.gov.in/) started from Arabian Sea to WG Mountain regions (Fig. 1b). It will now be fascinating to experiment the influence of hygroscopicity (κ) in the presence of convective clouds over that region.

The observation, methods, brief description of numerical simulation, WRF model parameterizations and experimental setup are presented in section 2. To investigate the role of aerosol hygroscopicity (κ) through two sensitivity tests, we have altered the model-prescribed κ values for the inorganics, and organic compositions. Section 3 describes the results, which is followed by discussion and conclusions in section 4.

2 Observations, Methods and Model descriptions

2.1 Observations

The variation of hygroscopicity (κ) in monsoon (JJAS) values with different dry aerosol sizes over High Altitude Cloud Physics Laboratory (HACPL), Mahabaleshwar, (India; 17.92 ^{o}N, 73.66 ^{o}E) is shown in Fig. 2 as obtained from HTDMA measurements. The measured low hygroscopicity (κ) values in the range of 0.1 to 0.25 are consistent and in good agreement with the observed isoprene generated secondary organic aerosol (SOA) over HACPL (Mukherjee et al. 2018). Ray et al. (2023) provide a thorough analysis of the average diurnal and seasonal variation in hygroscopicity over this region. Pringle et al. (2010) demonstrated that the average κ value in continental aerosols is 0.3, whereas in remote biogenic locations due, the κ value ranges between 0.15 and 0.22 (average value of 0.16) due to the predominance of organic aerosols (Levin et al. 2014). During the wet season in an Amazon tropical forest, kappa (κ) varied between 0.1 and 0.4 (average value of 0.16) (Gunthe et al. 2009). Pringle et al. (2010) have shown that marine aerosol is substantially more hygroscopic, with hygroscopicity of 0.72 due to large contributions from sea salts. Therefore, the location of WG mountains regions, particularly HACPL, Mahabaleshwar, may be predominated by both organic aerosols (κ ~ 0.1 – 0.3) in remote biogenic locations (like HACPL, Mahabaleshwar) and marine sea salt aerosols (κ ~ 0.5 – 1.4) from Arabian Sea during Indian summer monsoon due to large scale circulation. In this present study, we have used two different κ values (0.1 and 0.9) for the numerical simulations and regional climate model. The sensitivity model experiments are performed with different hygroscopicity (κ) values for a convective event over the Western Ghats.

2.2 Methods

The saturation ratio, S, over an aqueous solution droplet (Pruppacher and Klett, 1997; Chen, 1994), which considers both solute and curvature effect can be calculated from:

$$S = a_w exp\left(\frac{2\sigma_{ws}M_w}{RT\rho_w r}\right) \text{ -------------- (1)}$$

Where, a_w is the activity of water in the solution, ρ_w is the density of water, M_w is the molecular weight of water, σ_{ws} is the surface tension of the solution drop and air, R is the universal gas constant, T is temperature, and r is the wet radius of the droplet. The hygroscopicity parameter (kappa or κ) is related to the water activity of the solution as shown below (Petters and Kreidenweis, 2007):

$$\frac{1}{a_w} = 1 + \kappa\frac{V_s}{V_w} \text{ -------------- (2)}$$

Where, V_s is the volume of the dry particulate matter and V_w is the volume of the water. Therefore, the impacts of aerosol species on aerosol water content and cloud condensation nuclei (CCN) spectrum can be effectively predicted based on the modified Köhler theory or the revised κ-Köhler theory (Petters and Kreidenweis, 2007; Duan et al. 2019):

$$S = \frac{r^3 - r_d^3}{r^3 - r_d^3(1-\kappa)} exp\left(\frac{2\sigma_{ws} M_w}{RT\rho_w r}\right) \text{ -------------------- (3)}$$

Where, r_d is the dry aerosol radius. The hygroscopicity parameter (κ) can be obtained from HTDMA measurements situated at High Altitude Cloud Physics Laboratory (HACPL), Mahabaleshwar, (India; 17.92 ^{o}N, 73.66 ^{o}E). The above formula (Eq.3) is used in the numerical simulation for calculation of diffusional growth of cloud droplets. The brief description and mathematical formulation of numerical simulations are given in the following section 2.3 and details are shown in Bhowmik et al. (2023).

2.3 Brief description of numerical simulations and Weather Research Forecasting model

The droplet radius $r(X,t)$ was integrated from the diffusional droplet growth equation, which incorporates the solute and curvature effects (Korolev, 1995; Chen et al. 2020; Bhowmik et al. 2023),

$$\frac{dr(X,t)}{dt} = \frac{K}{r(X,t)+\xi}\left(S(X,t) + 1 - \left(\frac{r\,(X,t)^3 - r_d^3}{r(X,t)^3 - r_d^3(1-\kappa)} exp\left(\frac{2\sigma_{ws}}{R_v T \rho_w r(X,t)}\right)\right)\right) \text{ --------- (4)}$$

Here, κ is the hygroscopicity (for organic aerosols, κ = 0.1 and inorganics, κ = 0.9) and $\xi = \frac{\frac{D_v}{\alpha v} - K_1 \frac{k_T}{\omega v}}{1 + K_1}$. $K = \frac{D_v E}{\rho_w RT(1+K_1)}$, $K_1 = \left(\frac{L}{R_v T} - 1\right)\frac{L D_v E}{R_v T^2 k_T}$, D_v is the vapor diffusivity, R_v is the gas constant of water vapour, k_T is the thermal conductivity of air, α is the condensation coefficient, and ω is the thermal accommodation coefficient. The details can be found in Bhowmik et al. (2023).

Supersaturation in each grid cell is calculated as,

$$S(x,t) = \frac{E(x,t)}{E_s(x,t)} - 1 \qquad \text{------------ (5)}$$

and Water vapor pressure E(x,t) was calculated as

$$E = \frac{P q_v M_d}{q_v M_d + M_w} \quad \text{-----------} \ (6)$$

and the saturation water vapor pressure E_s(x,t) is calculated from the Clausian-Clapeyron equation.

It is important to mention here that the values of variables- latent heat of evaporation (L), the thermal conductivity of air, specific heat, the diffusivity of water vapor and all other related variables change with corresponding pressure, temperature, and height of the upward rising domain. The detailed discussion of the basic setup for the numerical simulation model is similar to Bhowmik et al. (2023) except for varying water activities or the values of hygroscopicity (κ).

The Advanced Weather Research and Forecasting (WRF-ARW) model version 4.0 developed by the National Center for Atmospheric Research is used for the sensitivity experiments. The simulations are performed considering four nested domains with a horizontal grid spacing of 27 (d01), 9 (d02), 3 (d03), and 1 (d04) km, respectively (Fig. 3). The model is initialized with the National Centre for Environmental Prediction Final operational global analysis data with 0.25° × 0.25° horizontal resolution (NCEP FNL) and 00 UTC initial conditions (IC). The Kain-Fritsch cumulus parameterization scheme is used only in the outer two domains (d01 & d02). The cloud-resolving third and fourth domains are treated with explicit convection. For microphysical parameterization, the aerosol-aware Thompson scheme (Thompson, and Eidhammer, 2014) is employed in all the simulations. For the idealized simulations, the model has been initialized in a single domain using the default input-sounding provided with the WRF for 2D squall line simulations (Morrison et al. 2009). The grid in both x and y directions is 149 points with a grid spacing of 1 km. All the physics options are turned off except for the microphysics. As the initialization is performed with an idealized input sounding, the simulated outputs are not compared with the observations.

3 Results

3.1 Role of hygroscopicity (κ) on CDSD using particle-by-particle based small-scale model simulations

Numerical simulation is an important tool to demonstrate and understand the growth of cloud droplets through diffusional growth processes, which consider both the solute effect (water activity or hygroscopicity) and curvature effect (detailed is discussed in Methods section 2.2). Figure 4 depicts the cloud droplet size distribution (CDSD) at different times from numerical simulation in a controlled environment. Using numerical simulation, we evaluate the impact of hygroscopicity (both for organic aerosols, $\kappa = 0.1$ and inorganics, $\kappa = 0.9$) on the nucleation mode ($r_d = 0.05$ μm) and accumulation mode ($r_d = 0.5$ μm) of aerosols. It is interesting to see the differences in CDSD from the initial mixing state (t = 2.5 sec) to well mixed state (t = 500 sec) due to changes in κ. The significant changes in CDSD in the smaller size bins (< 2.5 μm) are observed due to κ, whereas there are no changes in the larger bin sizes (> 12.5 μm) due to hygroscopicity (Fig. 4). For the clear look, we have zoomed the CDSD figures (Fig. 4c,d) in the smaller size bins. Moreover, numerical simulations show that nucleation mode ($r_d = 0.05$ μm) appears to be more important for submicron size (< 1 μm) smaller cloud droplet growth than accumulation mode ($r_d = 0.5$ μm) (Fig. 4). But there are no any significant changes between the CDSD spectra with organic and inorganic components. It is revealed that hygroscopicity (κ) modulates CDSD (i.e., growth of cloud droplets) from initial mixing state (t = 2.5 sec) to later well mixed state (t = 5 sec and more) in conjunction with two modes of aerosols (i.e., nucleation and accumulation). Regarding the influence of aerosol hygroscopicity, the numerical simulations clearly propose that the hygroscopicity of aerosol particles in the accumulation mode might be more important (Fig. 4b,d), which is similar to the recent study by Deng et al. (2022). The results from numerical simulations with hygroscopicity indicate the activation of smaller droplets, which may help for the cloud invigoration by uplifting below freezing level due to strong updraft and influence rain intensity. Therefore, direct numerical simulations can provide guidance and indicate the effect of cloud droplet growth processes due to changing κ. This understanding of cloud droplets growth due to hygroscopicity (kappa or κ) encourage to investigate in realistic atmospheric cloud for the change in rainfall intensity using regional climate model, such as WRF-ARW.

3.2 Role of hygroscopicity (κ) on CDSD, RDSD: Idealized WRF simulations

We also demonstrate the role of hygroscopicity by performing the 2D idealized simulations with various kappa (κ) values in Thomson microphysical scheme followed by the real case study simulations using the WRF model. In order to emphasize the significance of hygroscopicity (kappa or κ) on microphysical processes, simulations with 2D WRF, there are no planetary boundary layer, convective parameterization, surface layer scheme, longwave, and solar radiation schemes, are performed. The probability distributions of cloud hydrometeors (cloud and rain drops) are presented in Fig. 5 to demonstrate the influence of hygroscopicity (κ) on cloud microphysical diffusional growth. The idealized simulation, in which all physical processes are turned-off to avoid their interactions and feedback, is an essential experiment to prove the microphysical growth by κ. Therefore, the results of the drop size distributions of different cloud condensates (e.g., cloud and, rain droplets) due to changes in κ from 2D idealized simulations supports the significance of hygroscopicity on the cloud microphysical growth processes (Fig. 5). The density of cloud drop at bigger size (~ 9 micron) is more (less) in lower (higher) κ. On the other hand, in comparison to a less κ experiment, higher κ dominates in smaller sizes (~8 micron) cloud drop (Fig. 5a). It is interesting to note that the size distribution of raindrops has barely changed (Fig. 5b).

3.3 Role of hygroscopicity (κ) on cloud hydrometeors, rainfall and vertical velocity: WRF-ARW real simulations

Next, we evaluate the effect of hygroscopicity on the nucleation and accumulation mode separately and assess how these changes in hygroscopicity affect the hydrometeors. The hygroscopicity strongly influences the clouds in general and particularly different cloud hydrometeors (i.e., condensates), which might have impact on aerosol-cloud-radiation-precipitation feedbacks. We have selected two regions (i) near coastal region (R1) and, (ii) inland region, which is little far from the coast (R2) to understand the role of κ values on different types of clouds. The longitudinal variation (along the latitude of 18 ^{o}N) of model simulated radar reflectivity shows that cloud top height over region R1 is at 7 km, whereas it is at 12 km at the region R2 (Fig. 6). Therefore, the cloud over R2 is convective in nature (higher reflectivity along with height) as compared to R1 region (where reflectivity is less and height is less).

It is interesting to note that in both the regions (R1 and R2), less hygroscopicity (κ = 0.1, organics) simulates more cloud ice, snow and graupel (Fig. 7) as compared to more hygroscopicity (κ = 0.9, inorganics). Therefore, organic aerosols have a strong influence on the formation of more snow and graupel hydrometeors, which is irrespective of type of clouds (Fig. 7). The contribution of mixed-phase hydrometeors (i.e., snow and graupel) to the surface precipitation through melting process must depend on the size of those hydrometeors. In the R1 region, organic aerosol (lower value of κ) produces more snow and graupel and thereafter, rain hydrometeors (Fig. 7, 8). On the other hand, inorganic aerosol (higher value of κ) produces more rain and cloud mixing ratio (Fig. 8) over R2 region as compared to organic aerosols. In this case, organic aerosol produces high number but smaller size of snow and graupel particles as compared to inorganics and may therefore unable to contribute to the rain mixing ratio.

The cloud mixing ratio has no changes over R1 region due to hygroscopicity changes and the rain mixing ratio is slightly more in the case of low κ (Fig. 8a). Therefore, averaged surface rainfall is more (16.35 mm) due to low κ (organic aerosols) as compared to high κ (inorganic aerosols) (16.04 mm). It is also revealed that there are significant differences in the formation of both rain and cloud mixing ratios (Fig. 8a, b) in the R2 region, where high κ (inorganic aerosols) simulates more as compared to low κ (organic aerosols). Over the R2 region, the high κ produces more precipitation (7.3 mm) as compared to low κ (6.9 mm).

Hygroscopicity is also important to modify the simulation of vertical velocity (Fig. 8c, d). The vertical velocity is strongly influenced by the latent heat release of cloud hydrometeors during phase change and microphysical processes. The upper level strong updraft in the region R1 (convective core) by low κ is modulated by the strong latent heating as the formation of snow is more (Fig. 7). Due to the formation of more cloud and rain water mixing ratio over the same region, the middle level vertical velocity is more by high κ (Fig. 8a, b).

Fig. 9 reflects that more raindrops are scavenging to form of surface accumulated precipitation. The inorganic aerosols (kappa or κ = 0.9) has enhanced (suppressed) cloud and rain number concentrations compared to the organics (kappa or κ = 0.1) over the region R2 (R1). One-day accumulated rainfall from observation (IMD 0.25 deg. Gridded data) and two model sensitivity experiments (κ = 0.1 and κ = 0.9) are presented in Fig. 9a. Organic and inorganic aerosols produced rainfall are shown in Fig 9(b,c). There is no significant change in rainfall over coastal region (R1) (Fig 9a-c), we have separately zoomed the R2 region to demonstrate the change of spatial pattern and intensity of rainfall (Fig. 9d-f).

3.4 Number concentration of Cloud, Rain droplets and Precipitation due to hygroscopicity (κ): WRF-ARW real simulations

The results of the number concentration of rain and cloud droplets over two regions are presented in Fig. 10. Although, number concentrations of rain droplets do not change significantly, but substantial changes in cloud droplets number concentrations are noticed (Fig. 10). Therefore, CDSD from WRF simulations reveal that due to different κ values there are significant changes in the activation of smaller (< 10 μm) droplets (Figure not shown), which is consistent with direct numerical simulation (Fig. 4). As a result, the choices of hygroscopicity (κ) values are important for the growth of cloud droplets in realistic atmosphere and hence variations in the rainfall intensity. The smaller and higher number concentration of cloud droplets uplift below freezing level due to strong updraft in the convective environment and take part in the invigoration processes to intensify heavy rainfall over WG regions. The region R2 simulation with inorganic aerosols (κ = 0.9) has larger cloud (Fig. 8a, b), rain (Fig. 8a, b), and smaller snow and graupel (Fig. 7c, d) than organic aerosols (κ = 0.1). The strongest updrafts are found where cloud hydrometeors are more (Fig. 8c, d). Interestingly, in region R2, there are lower level strong vertical velocity due to inorganic aerosols and upper level strong vertical velocity due to organic aerosols (Fig. 8d). Further, we evaluate the changes in precipitation intensity and frequency distribution of rainfall intensity as simulated by WRF-ARW due to alterations of aerosol hygroscopicity values (Fig. 10, 11). There is significant change in rainfall intensity due to hygroscopicity, where increase or decrease of rainfall highly depends upon the type of clouds (i.e., shallow or deep). Hygroscopicity can influence the probability distribution of rainfall (Fig. 11). The inorganics aerosols (Kappa = 0.9) dominates in lower rain bins in both types of clouds (shallow, R1 and deep, R2). Surprisingly, in region R2, higher hygroscopicity simulates higher frequency of rainfall in all rain bins (Fig. 11). But, very importantly, in the shallow cloud (R1 regions), low hygroscopicity (κ = 0.1) dominates more rainfall frequency in higher rain bins (Fig. 11). Therefore, the presence of less hygroscopic aerosols (SOA) over Mahabaleshwar may be one of the reasons for getting heavy rainfall intensity (Fig. 11).

3.5 Role of nucleation and accumulation mode dry aerosol sizes composed with organics (low κ = 0.1) on cloud and precipitation

The sizes of dry aerosols are also important along with chemical composition for modifying the formation of cloud condensate as the growth of cloud droplets are different, which is also revealed in direct numerical simulation. Therefore, additional numerical simulations are conducted with WRF considering two modes of aerosols (nucleation, r_d = 0.05 μm and accumulation, r_d = 0.5 μm) in conjunction with organics composition (κ = 0.1). The observation from HTDMA results suggest the abundance of organics in the aerosol composition over the study region, which is also supported by previous study (Mukherjee et al., 2018). Figure 12 shows the area averaged mixing ratio of different cloud condensate for the same event (19th June, 2019) with two dry aerosol sizes composed with organics. It is fascinating to see the results in shallow clouds (region R1) and relatively deep clouds (region R2). In the region R, smaller (i.e., nucleation mode) and larger (i.e., accumulation mode) organic aerosols (κ = 0.1) have a similar influence on the production of cloud hydrometeors (Fig. 12a, c). In shallow clouds, there are no variations in the cloud water to total ice phase (the sum of the cloud ice, snow, and graupel) mixing ratio (Fig. 12a, c). The accumulation mode aerosols produce slightly less rain water as compared to the nucleation mode (Fig. 12a, c). In contracts, as demonstrated in Fig. 12 (b, d), organics composed nucleation mode (0.05 μm) aerosol in the deep cloud (region R2) can produce more total ice and rain water mass than larger aerosols (accumulation mode).

Cloud droplets produced by organics composed nucleation mode aerosols uplift below freezing level in the convective environment (R2 region) and able to yield more total ice phase hydrometeors (i.e., ice, snow and graupel) (Fig. 7b) and finally rain water mass (Fig. 8b, d). Like cloud water mass, number concentration of cloud droplets does not have significant changes for organics aerosols (Fig. 13). On the other hand, time evolution of rain droplet number concentrations varies with different dry aerosol sizes (Fig. 13) as revealed in the mass of rain water (Fig. 12). Therefore, the impact of curvature effect (Kelvin term) might vary depending on the types of clouds and hydrometeors.

4 **Discussions and Conclusions:**

We examine the two hygroscopicity values (low, 0.1 and high, 0.9) in the Thompson microphysics scheme of WRF during an event over the Western Ghats mountains to understand the role of the hygroscopicity on the simulation of cloud hydrometeors (such as ice, snow, graupel, cloud and, rain mixing ratio) and finally surface precipitation. The laboratory derived κ values and guided by direct numerical simulations with different hygroscopicity, we have conducted several sensitivity simulations using WRF in both idealized and real modes. Different hygroscopicity for individual aerosol composition with the varying aerosol sizes (nucleation and accumulation mode) drive the changes in microphysical characteristics (hydrometeors mass) that alter rainfall duration and intensity. Hygroscopicity can influence the spatial patterns of precipitation, the location of precipitation intensity and the probability distribution of rainfall.

Changing the hygroscopicity of inorganic aerosol species would have little effect in a region dominated by organic aerosol. The results conclude that the hygroscopicity is a good metric for distinguishing between inorganic (e.g., ammonium sulfate, and sodium chloride), and organic (e.g., SOA) aerosols. But it is very challenging for aerosols with complex compositions of inorganic and organic properties for the activation of droplets (Good et al. 2010). It is also worth noting that the aerosol hygroscopicity (kappa or κ) will activate differently in Aitken or nucleation and accumulation mode aerosols due to surface interactions effect (Pöhlker et al. 2021). These sensitivity experiments reveal that accumulated precipitation patterns, the duration and intensity of precipitation are sensitive to the representation of aerosol hygroscopicity within the WRF model. The drop concentrations of cloud condensate are presented using numerical simulation and Weather and Research Forecasting (WRF) model without chemistry.

Hygroscopicity value is important for severe weather event as shown by Saide et al. (2016), where they have demonstrated that a bulk hygroscopicity value of 0.4 potentially changes the significant tornado parameter. These results also highlight that misrepresentation of hygroscopicity values may therefore lead to unrealistic changes in the microphysics (formation of cloud hydrometeors) and precipitation patterns. In this study, we have not considered aerosols that act as ice nuclei (especially for dust and biological aerosol), which can impact the microphysical and radiation within convection (DeMott et al. 2003; Fan et al. 2013). In this present study, we have focused on the role of hygroscopicity primarily on the liquid phase (cloud and rain), and the ice phase (ice, snow and graupel), which affect precipitation.

Overall, these results suggest that the model treatment of aerosol composition via the hygroscopicity parameter can affect short-term weather and the simulation of cloud hydrometeors and probability density of rainfall in different categories. Including organic and inorganic aerosol hygroscopicity values leads to different realizations of hydrometeor formations and high-intensity precipitation. These differences suggest that future model studies in regions with varying aerosol compositions should pay closer attention to aerosol hygroscopicity.

Acknowledgements

We thank MoES, the Government of India, and the Director of IITM for all the support to carry out this work. We acknowledge Dr. Mahen Konwar for providing the CAIPEEX observational cloud droplets spectra used in the small-scale model. Authors thank Space Applications Center, ISRO, India Meteorological Department (IMD) for providing OLR and rainfall datasets respectively. We also thank the community of the freely available software (viz. NCAR Command Language (NCL), Ferret-NOAA, Climate Data Operators (CDO), and Origin Lab, Python). The authors would like to acknowledge the entire HACPL team regarding laboratory data analysis.

Data Availability Statement

All data used in this study are available kept in the following ftp link.

IP: 103.251.186.20; path: /home/JGR-atmosphere/Paper1; port: 21; user: JGR-atmosphere

pass: 2%Amn8i6@09

Declaration of Competing Interest

All authors declare that they have no known competing financial interests or personal relationships that could have appeared to influence the work reported in this paper.

CRediT authorship contribution statement

Avishek Ray: Methodology, WRF model simulations and analysis, Preparation of all data, Analysis, Writing -review & editing, Writing - original draft. **Moumita Bhowmik**: Methodology, Small-scale model simulations and analysis, Preparation of model data, Analysis, Writing -review & editing, Writing - original draft. **Anupam Hazra**: Conceptualization, Guiding, Methodology, WRF model data post-processing and Analysis, Writing - review & editing, Writing - original draft. **G. Pandithurai**: Guiding, Analysis, Writing – review & editing, Writing - original draft.

List of Figures Captions:

Figure 1: (a) The rainfall of 19th June 2019 from IMD gridded data. (b) Outgoing Long-wave Radiation (OLR) pattern for the same date of 19th June 2019 (Location of the HACPL, Mahabaleshwar is represented by the star mark).

Figure 2: Averaged aerosol hygroscopicity (κ) in Monsoon season observed by HTDMA at HACPL, Mahabaleswar, Western Ghats, India.

Figure 3: The domain setup (four nested domains) with a horizontal grid spacing of 27 (d01), 9 (d02), 3 (d03), and 1 (d04) km respectively.

Figure 4: The cloud droplets size distribution (CDSD) for nucleation (rd = 0.05 μm) and accumulation (rd = 0.5 μm) mode of aerosols in (a) and (b) respectively due to change of hygroscopicity (both for organic aerosols, κ = 0.1 and inorganics, κ = 0.9) at different time (from initial mixing state to well mix condition). The zoom of the (a) and (b) droplet activation and growth in smaller droplets are also shown in (c) and (d) for nucleation and accumulation mode aerosols respectively.

Figure 5: The probability density of cloud drop and rain drop sizes due to different hygroscopicity (Kappa = 0.1 and 0.9) from idealized WRF simulation.

Figure 6: The regions (R1 and R2) selected based on the (a) rainfall and (b) cloud formation as displayed from model simulated radar reflectivity.

Figure 7: The area averaged (a, b) total ice phase hydrometeors (i.e., sum of cloud ice, snow and graupel) and (c, d) snow and graupel mixing ratio over two regions (R1; Lon: 73.46-73.86 ^{o}E, Lat: 17.8-18.2 ^{o}N and R2; Lon: 74.6-75 ^{o}E, Lat: 17.8-18.2 ^{o}N) for two Kappa values (0.1 and 0.9).

Figure 8: The area averaged (a, b) cloud mixing ratio, rain mixing ratio and (c, d) vertical velocity over two regions (R1; Lon: 73.46-73.86 ^{o}E, Lat: 17.8-18.2 ^{o}N and R2; Lon: 74.6-75 ^{o}E, Lat: 17.8-18.2 ^{o}N) for two Kappa values (0.1 and 0.9).

Figure 9: (a-c) One-day accumulated rainfall from observation (IMD 0.25 deg. Gridded data) and two model sensitivity experiments (Kappa = 0.1 and Kappa = 0.9). (d-f) The spatial distributions of rainfall over R2 region due to hygroscopicity changes are presented.

Figure 10: The number concentration of cloud drop and rain drops due to different hygroscopicity (Kappa = 0.1 and 0.9) from real WRF simulation. The area averaged rainfalls due to hygroscopicity are also shown.

Figure 11: The probability distribution of rainfall over two regions due to different hygroscopicity (Kappa = 0.1 and 0.9) from real WRF simulation.

Figure 12: The area averaged (a, b) cloud mixing ratio, rain mixing ratio and (c, d) the area averaged total ice phase hydrometeors (i.e., sum of cloud ice, snow and graupel) over two regions (R1; Lon: 73.46-73.86 ^{o}E, Lat: 17.8-18.2 ^{o}N and R2; Lon: 74.6-75 ^{o}E, Lat: 17.8-18.2 ^{o}N) for organics (Kappa values = 0.1).

Figure 13: The number concentration of cloud drop and rain drops due to different dry aerosol sizes for organics (hygroscopicity, Kappa = 0.1) from real WRF simulation.

References

Bhowmik, M., Hazra, A., Rao, S. A. and Wang, L. P. (2023a) Eulerian-Lagrangian particle-based model for diffusional growth for the better parameterization of ISM clouds: A road map for improving climate model through small-scale model using observations. *Preprint*, DOI: 10.48550/arXiv.2303.00987.

Carrió, G. G., Cotton, W. R., & Cheng, W. Y. Y. (2010). Urban growth and aerosol effects on convection over Houston. Atmospheric Research, 96, 560–574.

Chen, S. and Xue, L. and Yau, M. K. (2020) Impact of aerosols and turbulence on cloud droplet growth: An in-cloud seeding case study using a parcel–DNS (direct numerical simulation) approach. Atmospheric Chemistry and Physics, 20, 10111–10124, DOI: https://doi.org/10.5194/acp-20-10111-2020.

Chen, J.-P., (1994). Theory of Deliquescence and Modified Köhler Curves. Journal of the Atmospheric Sciences, 51, 3505–3516. DOI: https://doi.org/10.1175/1520-0469(1994)051<3505:TODAMK>2.0.CO;2

Cheng, Y.F., Wiedensohler, A., Eichler, H., Heintzenberg, J., Tesche, M., Ansmann, A., Wendisch, M., Su, H., Althausen, D., Herrmann, H., Gnauk, T., Bruggemann, E., Hu, M., Zhang, Y.H., (2008). Relative humidity dependence of aerosol optical properties and direct radiative forcing in the surface boundary layer at Xinken in Pearl River Delta of China: an observation based numerical study. Atmospheric Environment, 42, 6373e6397.

DeMott, P. J., Sassen, K., Poellot, M. R., Baumgardner, D., Rogers, D. C., Brooks, S. D., … Kreidenweis, S. M. (2003). African dust aerosols as atmospheric ice nuclei. Geophysical Research Letters, 30, 1732. https://doi.org/10.1029/2003GL017410

Deng, Y., Fujinari, H., Yai, H., Shimada, K., …… Mochida, M., (2022). Offline analysis of the chemical composition and hygroscopicity of submicrometer aerosol at an Asian outflow receptor site and comparison with online measurements. Atmospheric Chemistry and Physics, 22, 5515–5533. https://doi.org/10.5194/acp-22-5515-2022

Duan, Y., Petters, M. D., & Barros, A. P., (2019). Understanding aerosol–cloud interactions through modeling the development of orographic cumulus congestus during IPHEx. Atmospheric Chemistry and Physics, 19, 1413–1437. https://doi.org/10.5194/acp-19-1413-2019.

Eidhammer, T., Morrison, H., Bansemer, A., Gettelman, A., & Heymsfield, A. J., (2014). Comparison of ice particle characteristics simulated by the Community Atmosphere Model (CAM5) with in-situ observations. Atmos. Chem. Phys. Discuss., 14, 7637–7681, www.atmos-chem-phys-discuss.net/14/7637/2014/

Fan, J., Leung, L. R., Rosenfeld, D., Chen, Q., Li, Z., Zhang, J., & Yan, H. (2013). Microphysical effects determine macrophysical response for aerosol impacts on deep convective clouds. Proceedings of the National Academy of Sciences of the United States of America, 110, E4581–E4590.

Farmer, D. K., Cappa, C. D., & Kreidenweis, S. M., (2015). Atmospheric processes and their controlling influence on cloud condensation nuclei activity. Chem. Rev., 115(10), 4199–4217, doi:10.1021/cr5006292.

Ghan, S. J., & Schwartz, S. E., (2007). Aerosol Properties and Processes: A Path from Field and Laboratory Measurements to Global Climate Models. Bulletin of the American Meteorological Society, 88, 1059–1084. DOI: https://doi.org/10.1175/BAMS-88-7-1059.

Good, N., Topping, D. O., Allan, J. D., Flynn, M., Fuentes, E., Irwin, M., … McFiggans, G. (2010). Consistency between parameterisations of aerosol hygroscopicity and CCN activity during the RHaMBLe discovery cruise. Atmospheric Chemistry and Physics, 10, 3189–3203.

Gunthe SS, King SM, Rose D, Chen Q, Roldin P, Farmer DK, et al., (2009). Cloud condensation nuclei in pristine tropical rainforest air of Amazonia: size-resolved measurements and modeling of atmo spheric aerosol composition and CCN activity. Atmos Chem Phys. 2009;9(19):7551–75. https://doi.org/10.5194/acp-9-7551-2009.

Kawecki, S., & Steiner, A. L. (2018). The influence of aerosol hygroscopicity on precipitation intensity during a mesoscale convective event. Journal of Geophysical Research: Atmospheres, 123, 424–442. https://doi.org/10.1002/2017JD026535

Khain, A. P., et al. (2015). Representation of microphysical processes in cloud-resolving models: Spectral (bin) microphysics versus bulk parameterization, Rev. Geophys., 53,247–322, doi:10.1002/2014RG000468.

Konwar M., Das S.K., Deshpande S.M., Chakravarty K., Goswami B. N., (2014). Microphysics of clouds and rain over the Western Ghat. Journal of Geophysical Research, 119, 1-20, DOI:10.1002/2014JD021606.

Korolev, A. V. (1995) The Influence of Supersaturation Fluctuations on Droplet Size Spectra Formation. Journal of the Atmospheric Sciences, 52,3620–3634, DOI: 10.1175/1520-0469(1995)052<3620:TIOSFO>2.0.CO;2.

Kumar, S., Hazra A., Goswami B.N., (2014). Role of interaction between dynamics, thermodynamics and cloud microphysics on summer monsoon precipitating clouds over the Myanmar Coast and the Western Ghats. Climate Dynamics, 43, 911-924, DOI:10.1007/s00382-013-1909-3.

Levin EJT, Prenni AJ, Palm BB, Day DA, Campuzano-Jost P, Winkler PM, et al. (2014). Size-resolved aerosol composition and its link to hygroscopicity at a forested site in Colorado. Atmos Chem Phys. 2014;14(5):2657–67. https://doi.org/10.5194/acp-14-2657-2014.

Maheskumar R. S., Narkhedkar S. G., Morwal S. B., Padmakumari B., Kothawale D. R., Joshi R. R., Deshpande C. G., Bhalwankar R. V., Kulkarni J. R., (2014). Mechanism of high rainfall over the Indian west coast region during the monsoon season. Climate Dynamics, 43, 1513-1529, DOI:10.1007/s00382-013-1972-9

Mandariya, A. K., Gupta, T., Tripathi, S. N., (2019). Effect of aqueous-phase processing on the formation and evolution of organic aerosol (OA) under different stages of fog life cycles. Atmospheric Environment, 206, 60-71. https://doi.org/10.1016/j.atmosenv.2019.02.047

Malm, W.C., Day, D., Carrico, C. M., Kreidenweis, S. M., Collett, J., McMeeking, G., Lee, T., Carrillo, J., (2005). Intercomparison and closure calculations using measurements of aerosol species and optical properties during the Yosemite Aerosol Characterization study Journal Geophysical Resarch, 110, D14302. 10.1029/2004JD005494

Morrison, H., Thompson, G., & Tatarskii, V., (2009). Impact of cloud microphysics on the development of trailing stratiform precipitation in a simulated squall line: Comparison of one- and two-moment schemes. Mon. Wea. Rev., 137 , 991–1007.

Mukherjee S., Singla V., Pandithurai G., Safai P.D., Meena G.S., Dani K.K., Anil Kumar V., (2018). Seasonal variability in chemical composition and source apportionment of sub-micron aerosol over a high altitude site in Western Ghats, India. Atmospheric Environment, 180, 79-92. DOI:10.1016/j.atmosenv.2018.02.048.

Parthasarathy, B., Munot, A. A., & Kothawale, D. R., (1994). All-India monthly and seasonal rainfall series: 1871–1993. Theoretical and Applied Climatology, 49, 217–224. https://doi.org/10.1007/BF00867461

Petters, M. D., & Kreidenweis, S. M., (2007). A single parameter representation of hygroscopic growth and cloud condensa tion nucleus activity. Atmos. Chem. Phys., 7, 1961–1971. https://doi.org/10.5194/acp-7-1961-2007.

Petters, M. D., & Kreidenweis, S. M., (2008). A single parameter repre sentation of hygroscopic growth and cloud condensation nucleus activity Part 2: Including solubility, Atmospheric Chemistry and Physics, 8, 6273–6279, doi:10.5194/acp-8-6273-2008.

Pringle, K. J., Tost, H., Pozzer, A., Poschl, U., Lelieveld, J., (2010). Global distribution of the effective aerosol hygroscopicity parameter for CCN activation. Atmospheric Chemistry and Physics, 10, 5241-5255.

Pruppacher, H. R. and Klett, J. D.: Microphysics of Clouds and Precipitation, Kluwer Acad., Norwell, Mass., 442–443 (chap. 10), 1997.

Pöhlker, M. L., Zhang, M., Campos Braga, R., Krüger, O. O., Pöschl, U., and Ervens, B., (2021). Aitken mode particles as CCN in aerosol- and updraft-sensitive regimes of cloud droplet formation, Atmos. Chem. Phys., 21, 11723–11740, https://doi.org/10.5194/acp-21-11723-2021.

Randall, D.A., Wood, R.A., Bony, S., Colman, R., et al. (2007). Climate models and their evaluation. In Climate change 2007: The physical science basis. Contribution of Working Group I to the Fourth Assessment Report of the IPCC (FAR) (pp. 589–662). Cambridge University Press.

Rosenfeld, D., Lohmann, U., ……. Andreae, M. O., (2008), Flood or drought: how do aerosols affect precipitation. Science, 321, 1309–1313. DOI: 10.1126/science.1160606

Saide, P. E., Thompson, G., Eidhammer, T., Silva, A. M., Pierce, R. B., & Carmichael, G. R. (2016). Assessment of biomass burning smoke influence on environmental conditions for multiyear tornado outbreaks by combining aerosol-aware microphysics and fire emission constraints. Journal of Geophysical Research: Atmospheres, 121, 10,294–10,311. https://doi.org/10.1002/2016JD025056

Slowik, J. G., Vlasenko, A., McGuire, M., Evans, G. J., and Abbatt, J. P. D., (2010). Simultaneous factor analysis of organic particle and gas mass spectra: AMS and PTR-MS measurements at an urban site. Atmospheric Chemistry and Physics, 10, 1969–1988, doi:10.5194/acp-10-1969-2010.

Tang, I. N., & Munkelwitz, H. R., (1994). Water Activities, Densities, and Refractive-Indexes of Aqueous Sulfates and Sodium-Nitrate Droplets of Atmospheric Importance, J. Geophys. Res.-Atmos., 99, 18801–18808, https://doi.org/10.1029/94jd01345.

Thompson, G., & Eidhammer, T. (2014). A study of aerosol impacts on clouds and precipitation development in a large winter cyclone. Journal of the Atmospheric Sciences, 71(10), 3636–3658. https://doi.org/10.1175/JAS-D-13-0305.1

Van der Heever, S. C., Carrió, G. G., Cotton, W. R., DeMott, P. J., & Prenni, A. J. (2006). Impacts of nucleating aerosol on Florida storms. Part I: Mesoscale simulations. Journal of the Atmospheric Sciences, 63, 1752–1775.

Vlasenko, A., Slowik, J. G., Bottenheim, J., Brickell, P., Chang, R.- W., Macdonald, A., Shantz, N., Sjostedt, S., Wiebe, H., Leaitch, W., and Abbatt, J., (2009). Measurements of VOCs by Proton-Transfer Reaction Mass Spectrometry at a Rural Ontario Site: Sources and Correlation to Aerosol Composition. Journal of Geophysical Research, 114, D21305, doi:10.1029/2009JD012025.

Wang, Y., Li, Z., Zhang, Y., Du, W., Zhang, F., Tan, H., Xu, H., Fan, T., Jin, X., Fan, X., Dong, Z., Wang, Q., and Sun, Y., (2018). Characterization of aerosol hygroscopicity, mixing state, and CCN activity at a suburban site in the central North China Plain, Atmos. Chem. Phys., 18, 11739–11752, https://doi.org/10.5194/acp-18-11739-2018.

List of Figures:

Figure 1: (a) The rainfall of 19th June 2019 from IMD gridded data. (b) Outgoing Long-wave Radiation (OLR) pattern for the same date of 19th June 2019 (Location of the HACPL, Mahabaleshwar is represented by the star mark).

Figure 2: Averaged aerosol hygroscopicity (κ) in Monsoon season observed by HTDMA at HACPL, Mahabaleswar, Western Ghats, India.

Figure 3: The domain setup (four nested domains) with a horizontal grid spacing of 27 (d01), 9 (d02), 3 (d03), and 1 (d04) km respectively.

Figure 4: The cloud droplets size distribution (CDSD) for nucleation (r_d = 0.05 μm) and accumulation (r_d = 0.5 μm) mode of aerosols in (a) and (b) respectively due to change of hygroscopicity (both for organic aerosols, κ = 0.2 and inorganics, κ = 0.9) at different time (from initial mixing state to well mix condition). The zoom of the (a) and (b) droplet activation and growth in smaller droplets are also shown in (c) and (d) for nucleation and accumulation mode aerosols respectively.

Figure 5: The probability density of cloud drop and rain drop sizes due to different hygroscopicity (Kappa = 0.1 and 0.9) from idealized WRF simulation.

Figure 6: The regions (R1 and R2) selected based on the (a) rainfall and (b) cloud formation as displayed from simulated radar reflectivity.

Figure 7: The area averaged (a, b) total ice phase hydrometeors (i.e., sum of cloud ice, snow and graupel) and (c, d) snow and graupel mixing ratio over two regions (R1; Lon: 73.46-73.86 ^{o}E, Lat: 17.8-18.2 ^{o}N and R2; Lon: 74.6-75 ^{o}E, Lat: 17.8-18.2 ^{o}N) for two Kappa values (0.1 and 0.9).

Figure 8: The area averaged (a, b) cloud mixing ratio, rain mixing ratio and (c, d) vertical velocity over two regions (R1; Lon: 73.46-73.86 ^{o}E, Lat: 17.8-18.2 ^{o}N and R2; Lon: 74.6-75 ^{o}E, Lat: 17.8-18.2 ^{o}N) for two Kappa values (0.1 and 0.9).

Figure 9: (a-c) One-day accumulated rainfall from observation (IMD 0.25 deg. Gridded data) and two model sensitivity experiments (Kappa = 0.1 and Kappa = 0.9). (d-f) The spatial distributions of rainfall over R2 region due to hygroscopicity changes are presented.

Figure 10: The number concentration of cloud drop and rain drops due to different hygroscopicity (Kappa = 0.1 and 0.9) from real WRF simulation. The area averaged rainfalls due to hygroscopicity are also shown.

Figure 11: The probability distribution of rainfall over two regions due to different hygroscopicity (Kappa = 0.1 and 0.9) from real WRF simulation.

Figure 12: The area averaged (a, b) cloud mixing ratio, rain mixing ratio and (c, d) the area averaged total ice phase hydrometeors (i.e., sum of cloud ice, snow and graupel) over two regions (R1; Lon: 73.46-73.86 ^{o}E, Lat: 17.8-18.2 ^{o}N and R2; Lon: 74.6-75 ^{o}E, Lat: 17.8-18.2 ^{o}N) for organics (Kappa values = 0.1).

Figure 13: The number concentration of cloud drop and rain drops due to different dry aerosol sizes for organics (hygroscopicity, Kappa = 0.1) from real WRF simulation.

Figures:

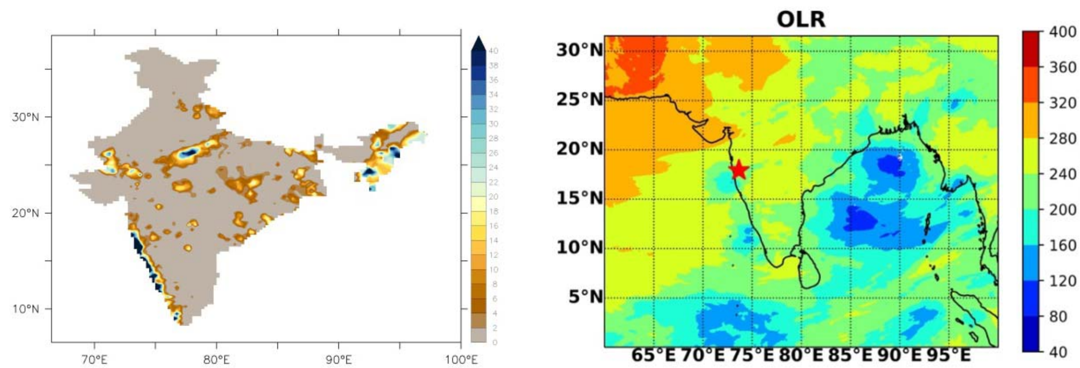

Figure 1: (a) The rainfall of 19th June 2019 from IMD gridded data. (b) Outgoing Long-wave Radiation (OLR) pattern for the same date of 19th June 2019 (Location of the HACPL, Mahabaleshwar is represented by the star mark).

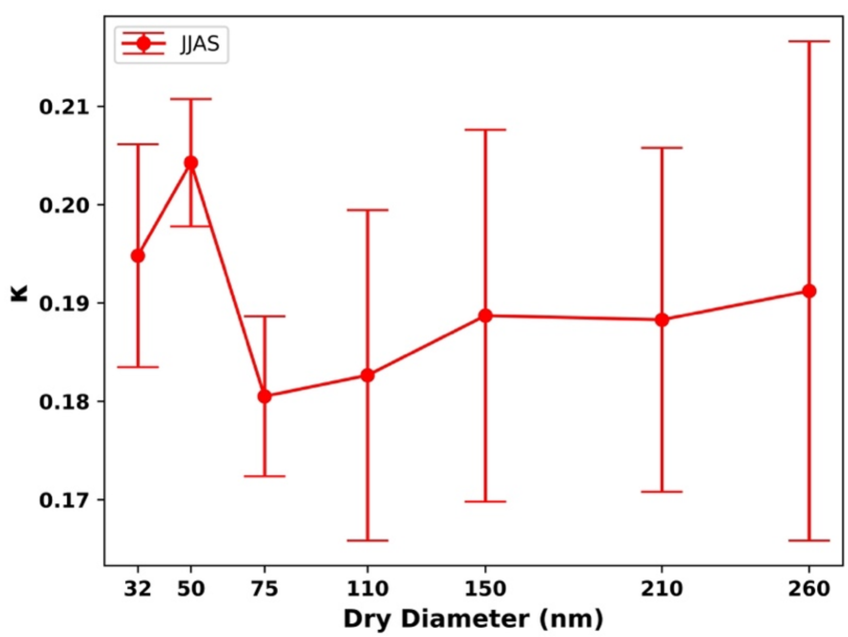

Figure 2: Averaged aerosol hygroscopicity in Monsoon season observed by HTDMA at HACPL.

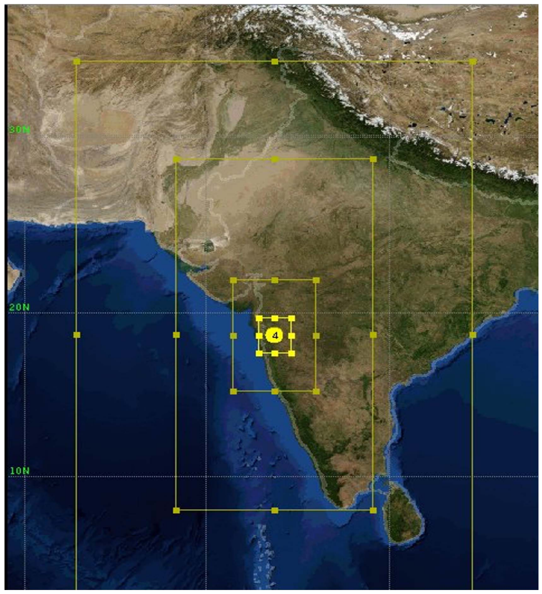

Figure 3: The domain setup (four nested domains) with a horizontal grid spacing of 27 (d01), 9 (d02), 3 (d03), and 1 (d04) km respectively.

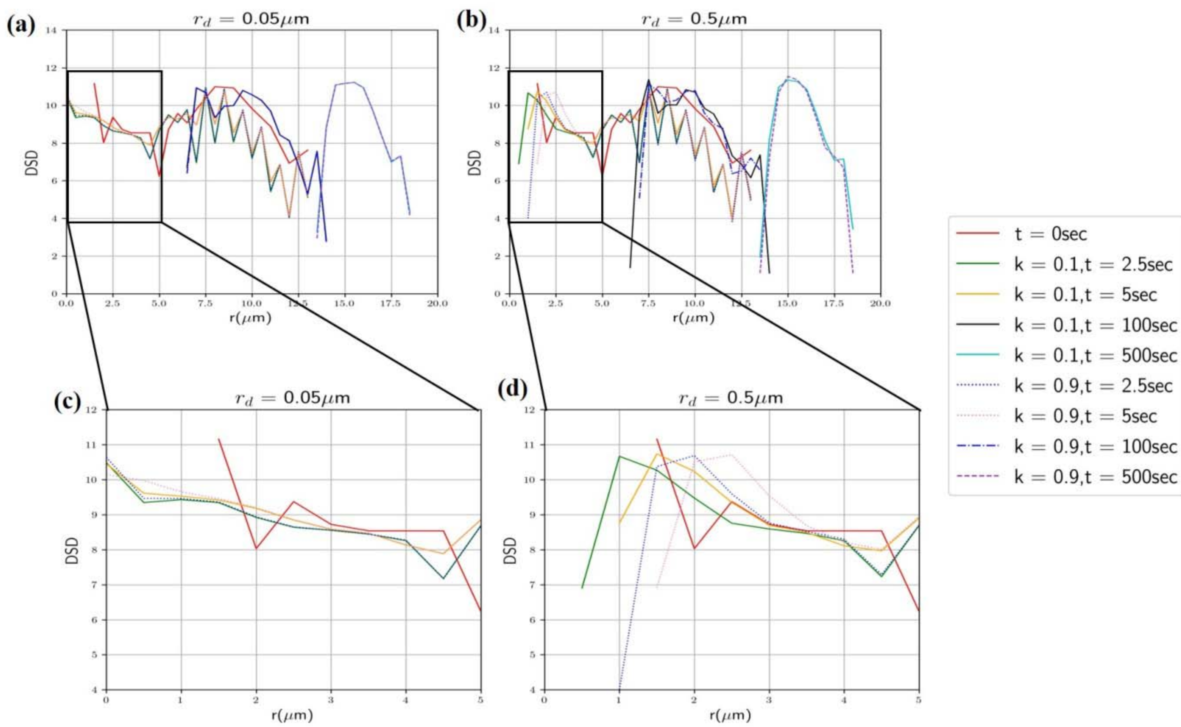

Figure 4: The cloud droplets size distribution (CDSD) for nucleation (r_d = 0.05 μm) and accumulation (r_d = 0.5 μm) mode of aerosols in (a) and (b) respectively due to change of hygroscopicity (both for organic aerosols, κ = 0.1 and inorganics, κ = 0.9) at different time (from initial mixing state to well mix condition). The zoom of the (a) and (b) droplet activation and growth in smaller droplets are also shown in (c) and (d) for nucleation and accumulation mode aerosols respectively.

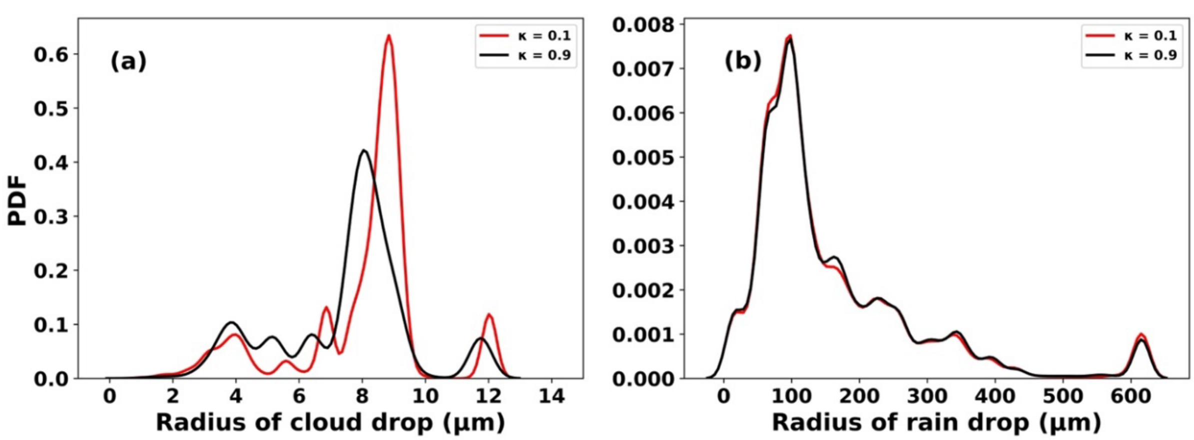

Figure 5: The probability density of cloud drop and rain drop sizes due to different hygroscopicity (Kappa = 0.1 and 0.9) from idealized WRF simulation.

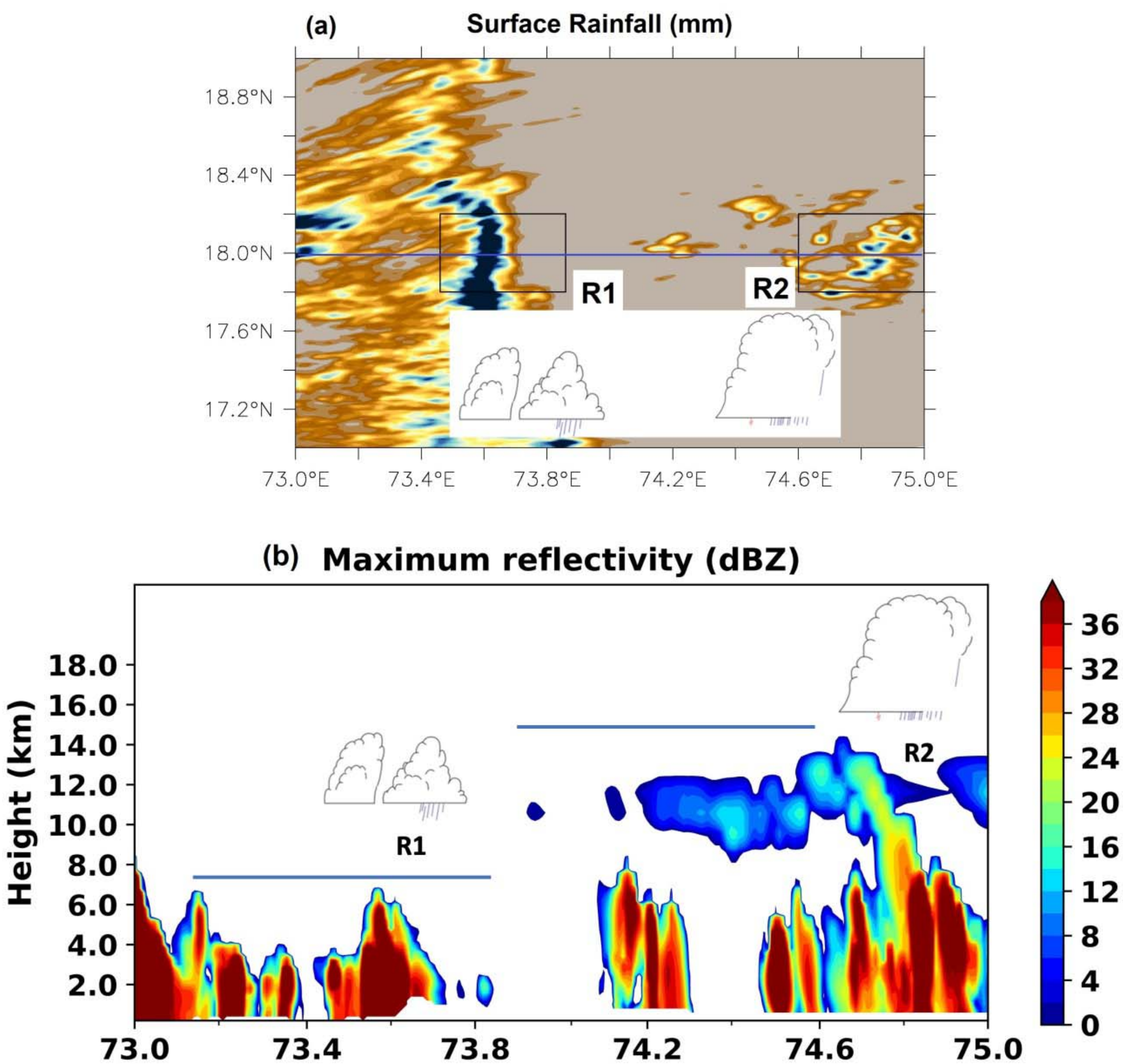

Figure 6: The regions (R1 and R2) selected based on the (a) rainfall and (b) cloud formation as displayed from model simulated radar reflectivity.

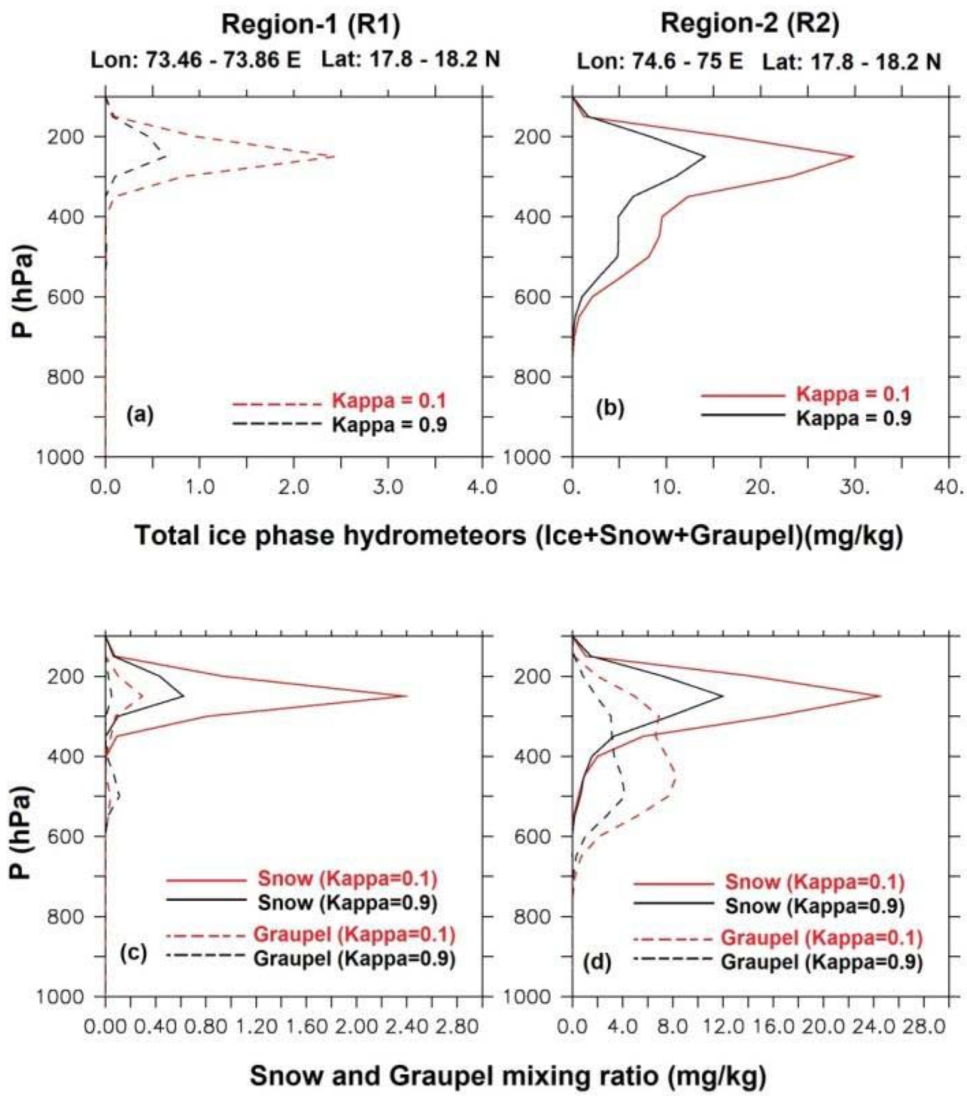

Figure 7: The area averaged (a, b) total ice phase hydrometeors (i.e., sum of cloud ice, snow and graupel) and (c, d) snow and graupel mixing ratio over two regions (R1; Lon: 73.46-73.86 ^{o}E, Lat: 17.8-18.2 ^{o}N and R2; Lon: 74.6-75 ^{o}E, Lat: 17.8-18.2 ^{o}N) for two Kappa values (0.1 and 0.9).

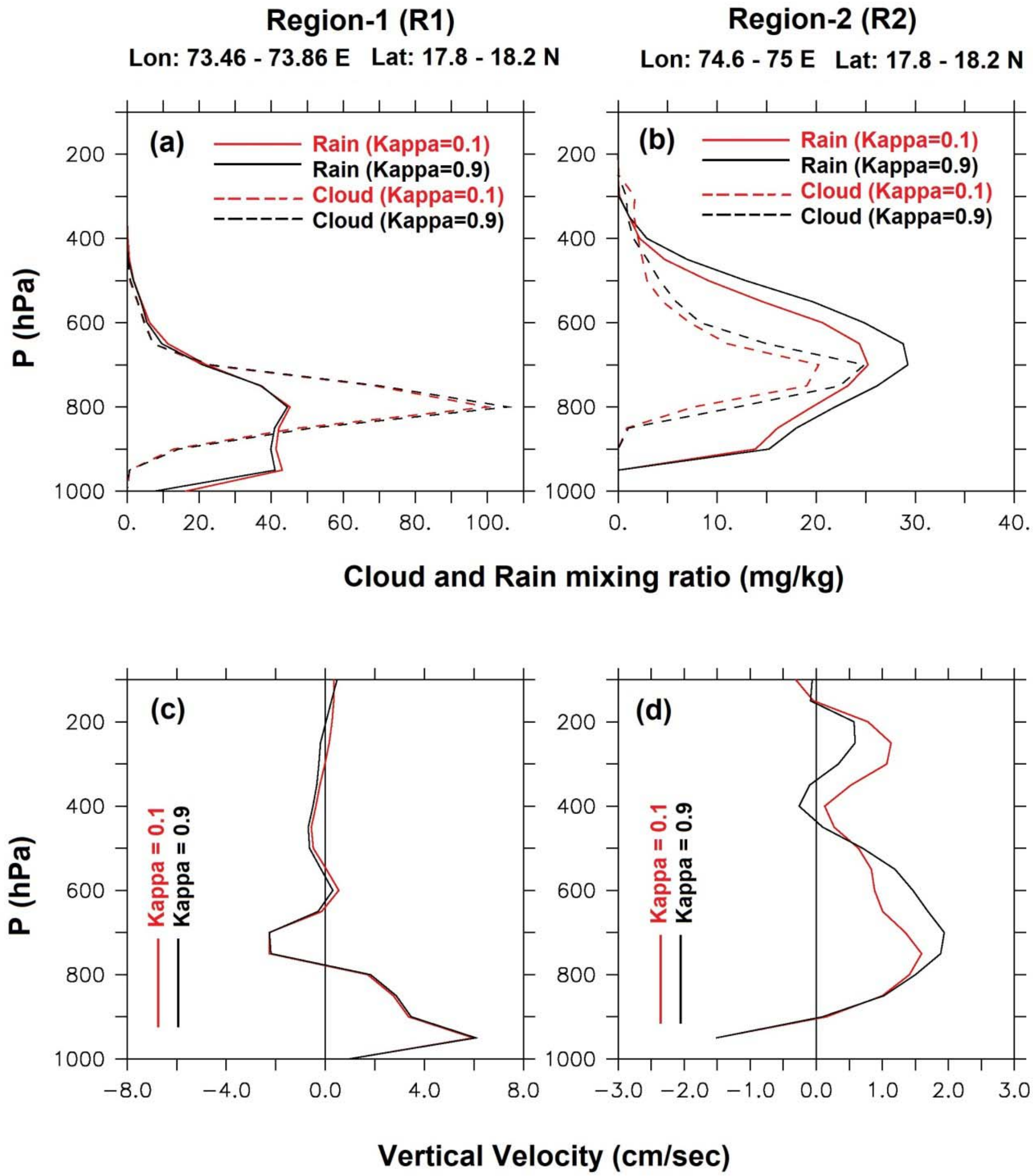

Figure 8: The area averaged (a, b) cloud mixing ratio, rain mixing ratio and (c, d) vertical velocity over two regions (R1; Lon: 73.46 -73.86 ^{o}E, Lat: 17.8 - 18.2 ^{o}N and R2; Lon: 74.6 – 75 ^{o}E, Lat: 17.8 - 18.2 ^{o}N) for two Kappa values (0.1 and 0.9).

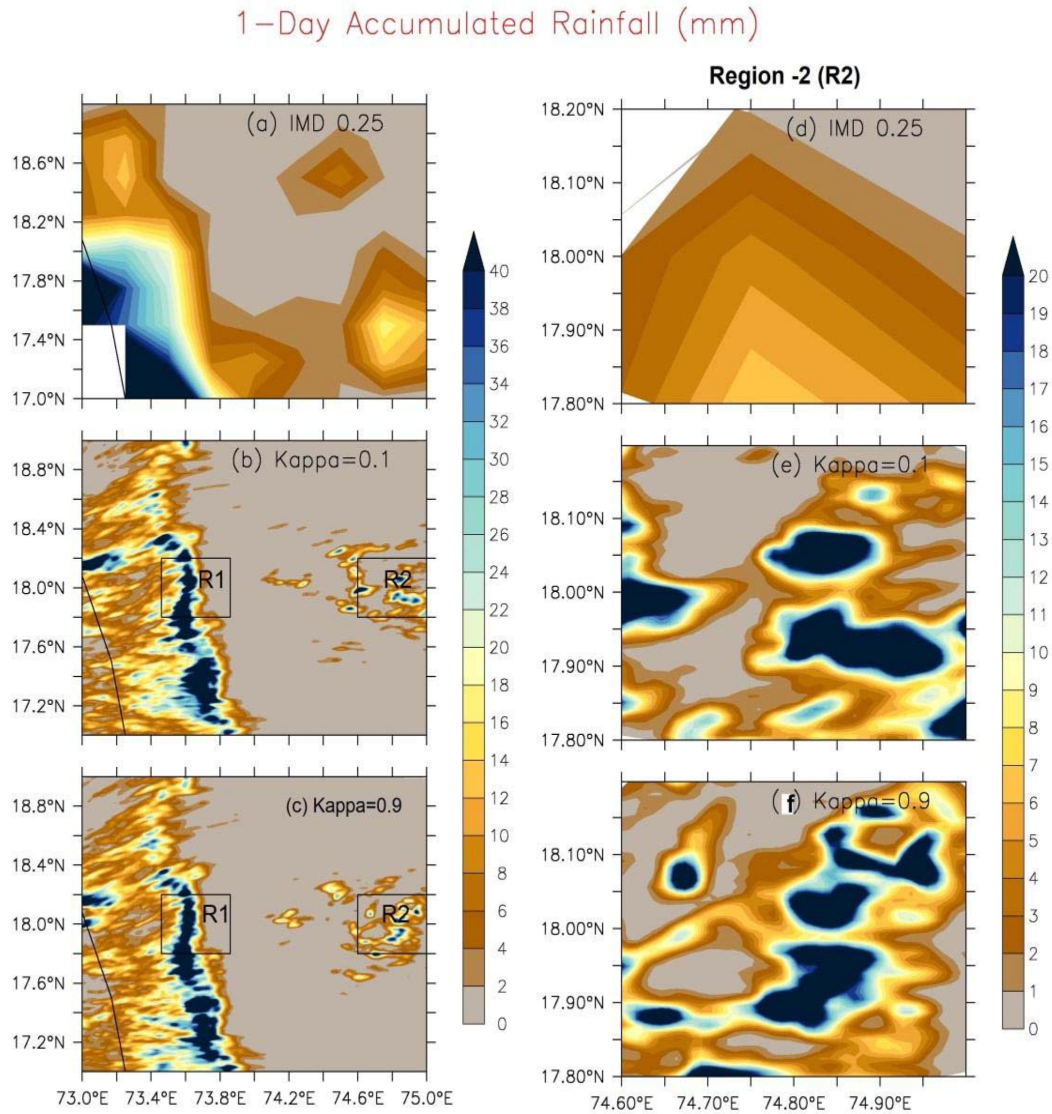

Figure 9: (a-c) One-day accumulated rainfall from observation (IMD 0.25 deg. Gridded data) and two model sensitivity experiments (Kappa = 0.1 and Kappa = 0.9). (d-f) The spatial distributions of rainfall over R2 region due to hygroscopicity changes are presented.

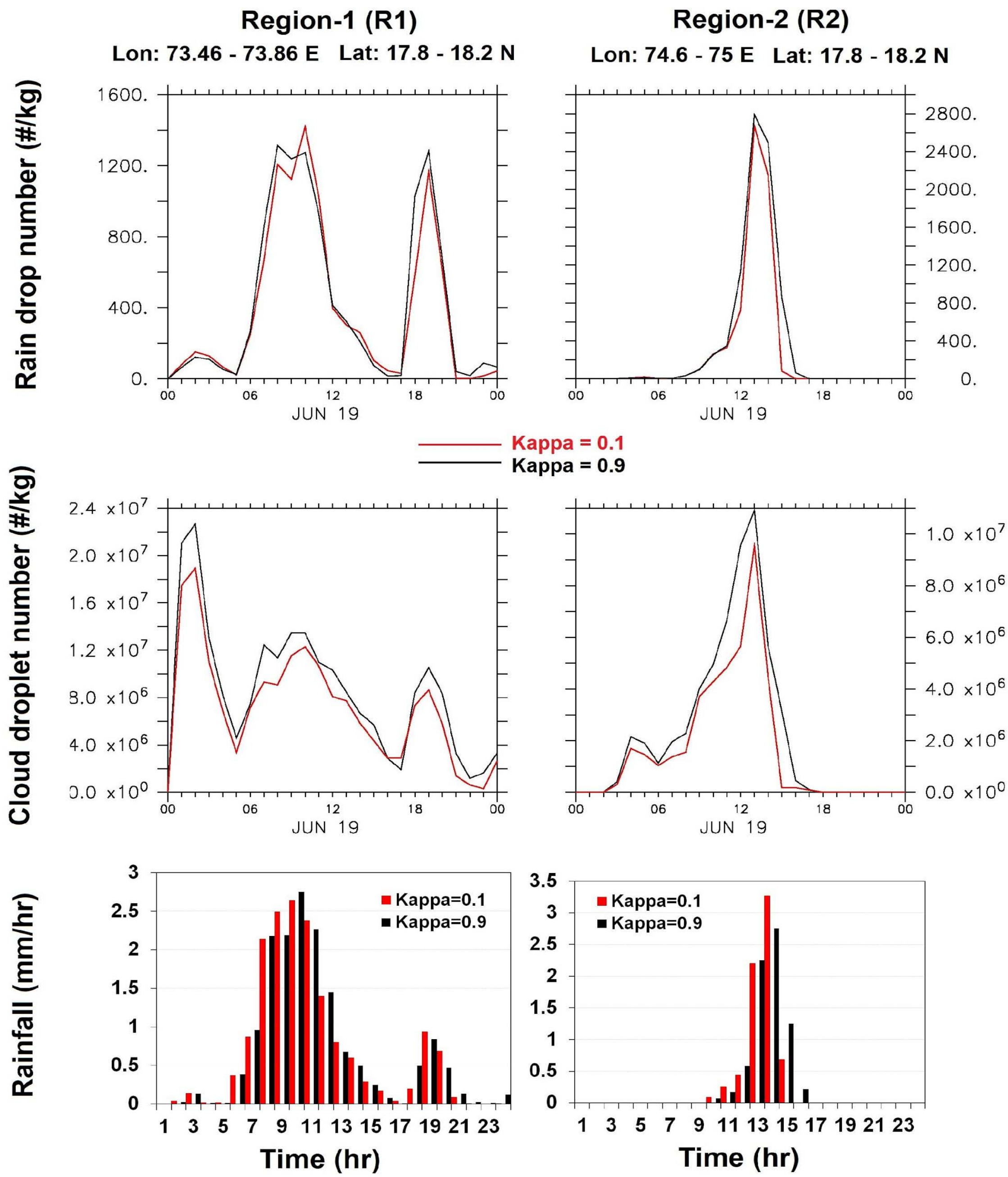

Figure 10: The number concentration of cloud drop and rain drops due to different hygroscopicity (Kappa = 0.1 and 0.9) from real WRF simulation. The area averaged rainfall due to hygroscopicity is also shown.

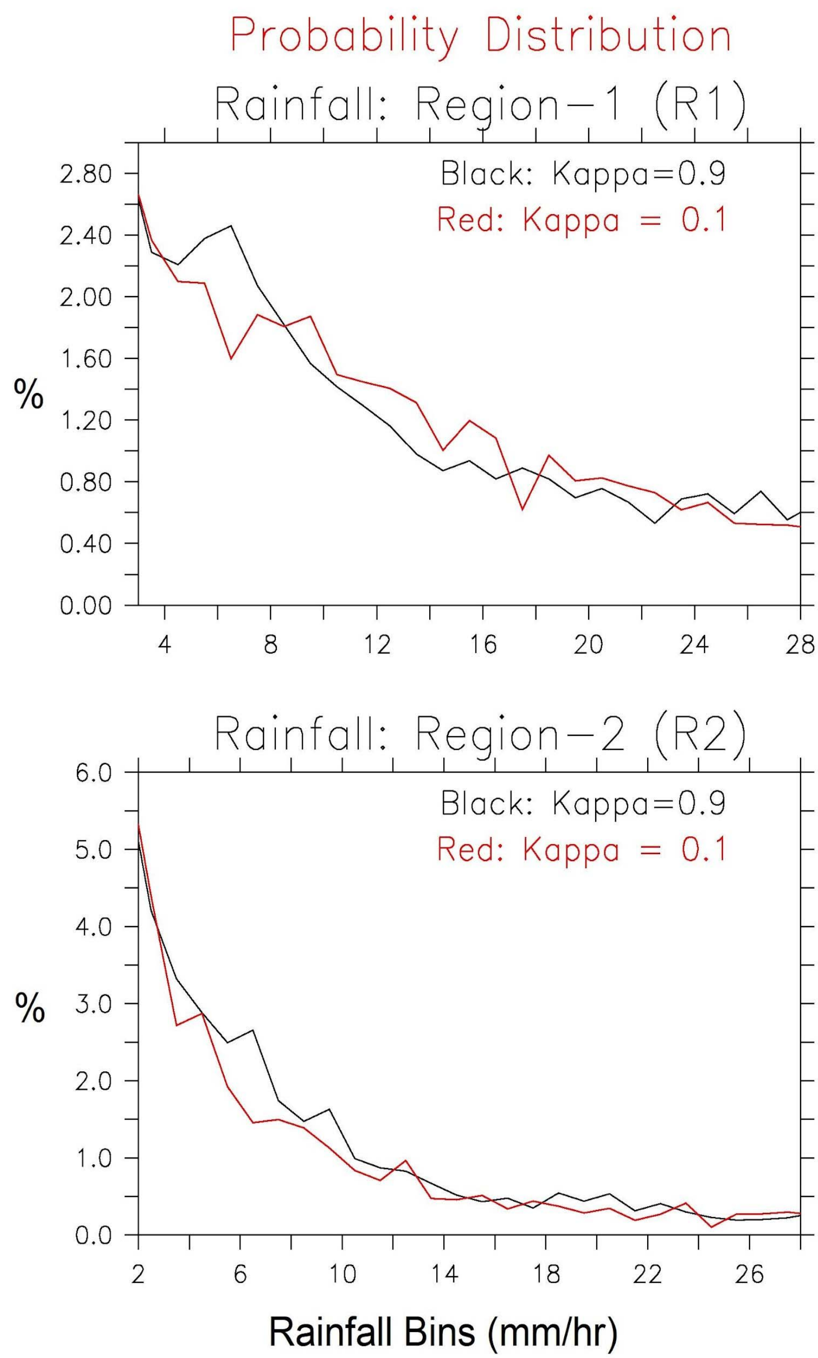
Probability Distribution
Rainfall: Region−1 (R1)
Black: Kappa=0.9
Red: Kappa = 0.1
%
2.80
2.40
2.00
1.60
1.20
0.80
0.40
0.00
4
8
12
16
20
24
28
Rainfall: Region−2 (R2)
Black: Kappa=0.9
Red: Kappa = 0.1
%
6.0
5.0
4.0
3.0
2.0
1.0
0.0
2
6
10
14
18
22
26
Rainfall Bins (mm/hr)

Figure 11: The probability distribution of rainfall over two regions due to different hygroscopicity (Kappa = 0.1 and 0.9) from real WRF simulation.

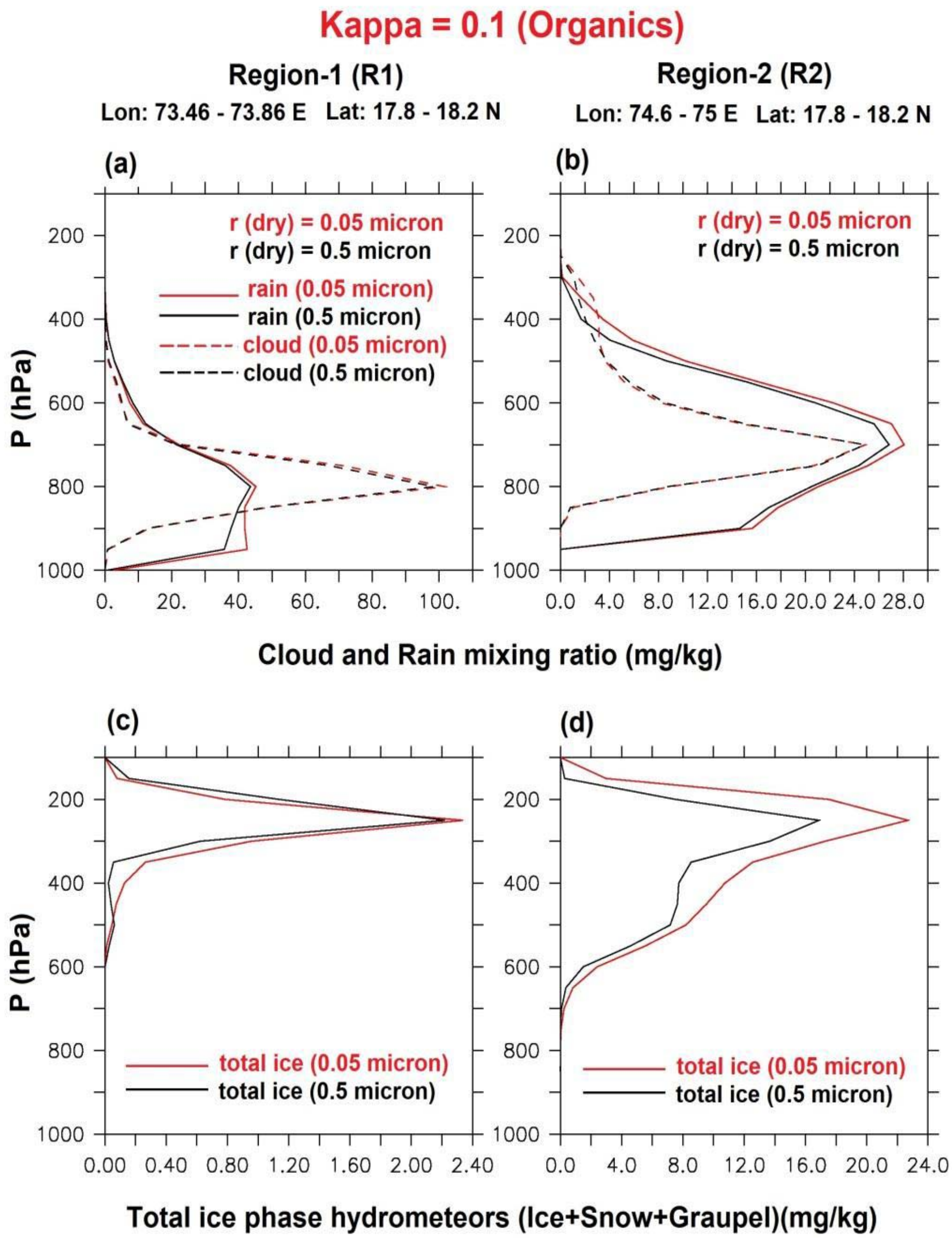

Figure 12: The area averaged (a, b) cloud mixing ratio, rain mixing ratio and (c, d) the area averaged total ice phase hydrometeors (i.e., sum of cloud ice, snow and graupel) over two regions (R1; Lon: 73.46 - 73.86 ^{o}E, Lat: 17.8 - 18.2 ^{o}N and R2; Lon: 74.6 – 75 ^{o}E, Lat: 17.8 - 18.2 ^{o}N) for organics (Kappa values = 0.1).

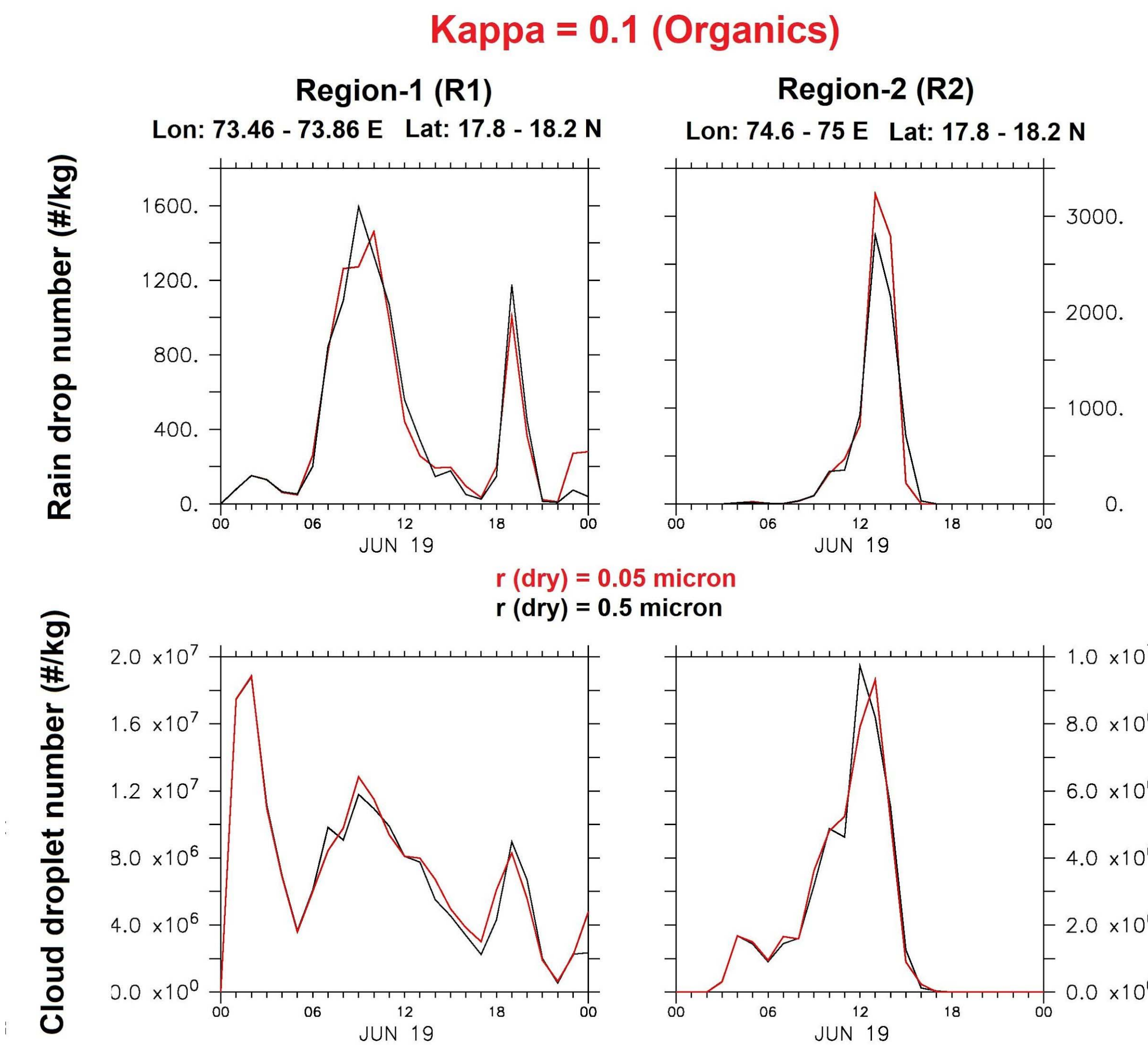

Figure 13: The number concentrationof cloud drop and rain drops due to different dry aerosol sizes for organics (hygroscopicity, Kappa = 0.1) from real WRF simulation.

Figure 1.

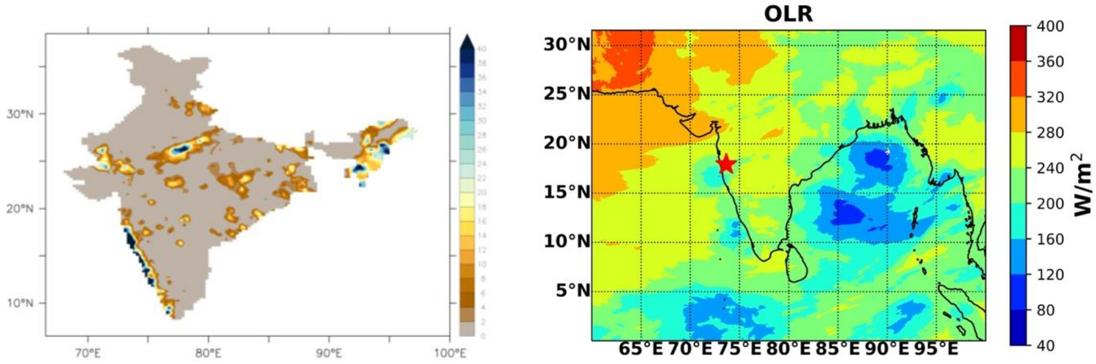
30°N
20°N
10°N
70°E
80°E
90°E
100°E
OLR
30°N
25°N
20°N
15°N
10°N
5°N
65°E 70°E 75°E 80°E 85°E 90°E 95°E
400
360
320
280
240
200
160
120
80
40
W/m^2

Figure 1:

Figure 2.

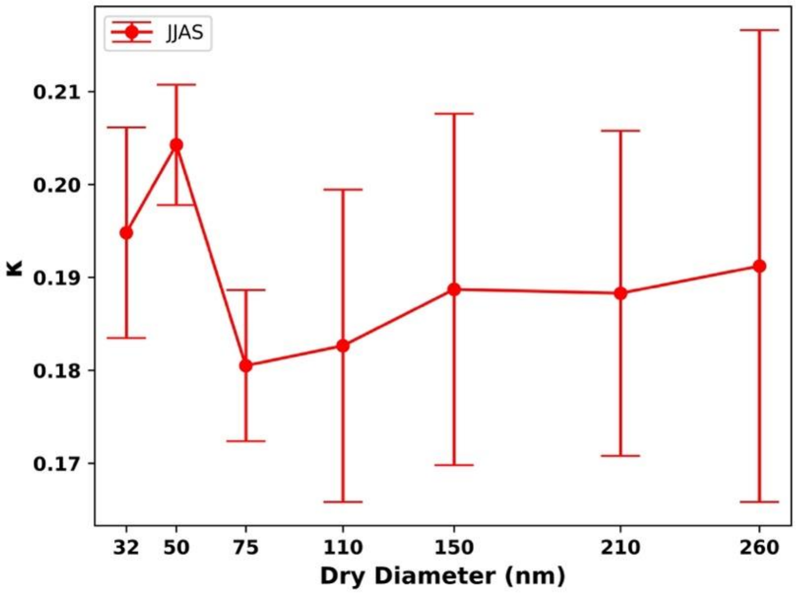
JJAS
K
0.21
0.20
0.19
0.18
0.17
32
50
75
110
150
210
260
Dry Diameter (nm)

Figure 2:

Figure 3.

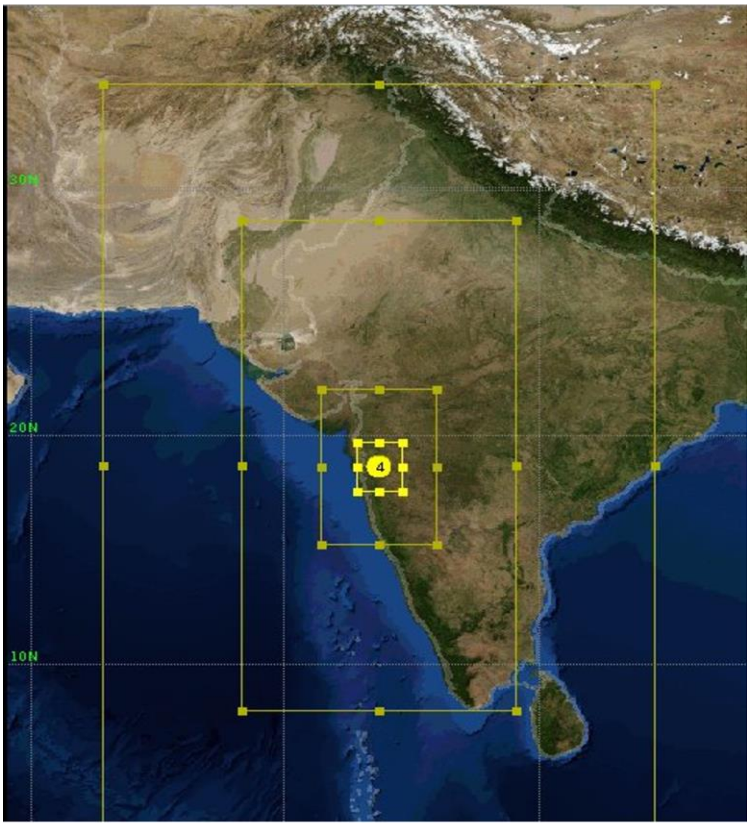

Figure 3:

Figure 4.

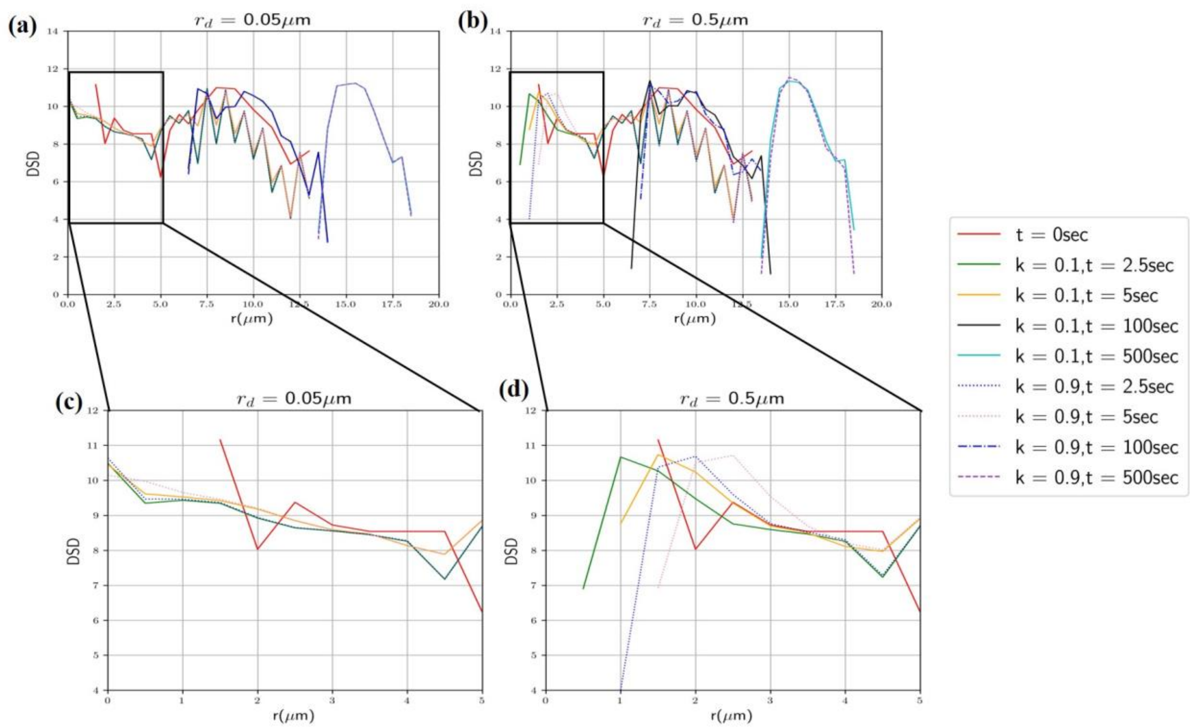

(a)
$r_d = 0.05\mu m$
(b)
$r_d = 0.5\mu m$
(c)
$r_d = 0.05\mu m$
(d)
$r_d = 0.5\mu m$
DSD
r(μm)
t = 0sec
k = 0.1,t = 2.5sec
k = 0.1,t = 5sec
k = 0.1,t = 100sec
k = 0.1,t = 500sec
k = 0.9,t = 2.5sec
k = 0.9,t = 5sec
k = 0.9,t = 100sec
k = 0.9,t = 500sec

Figure 4

Figure 5.

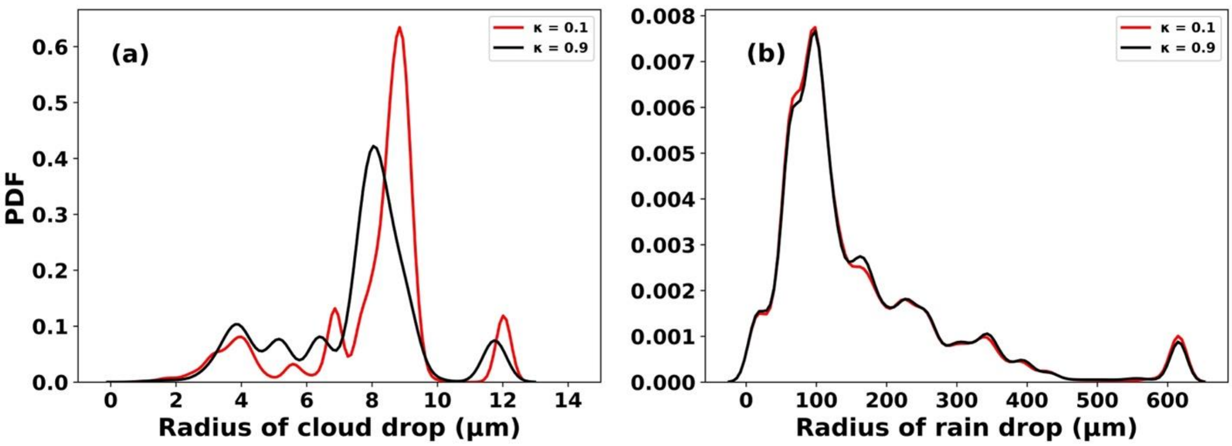

(a)
κ = 0.1
κ = 0.9
PDF
0.0
0.1
0.2
0.3
0.4
0.5
0.6
0
2
4
6
8
10
12
14
Radius of cloud drop (μm)
(b)
κ = 0.1
κ = 0.9
0.000
0.001
0.002
0.003
0.004
0.005
0.006
0.007
0.008
0
100
200
300
400
500
600
Radius of rain drop (μm)

Figure 5:

Figure 6.

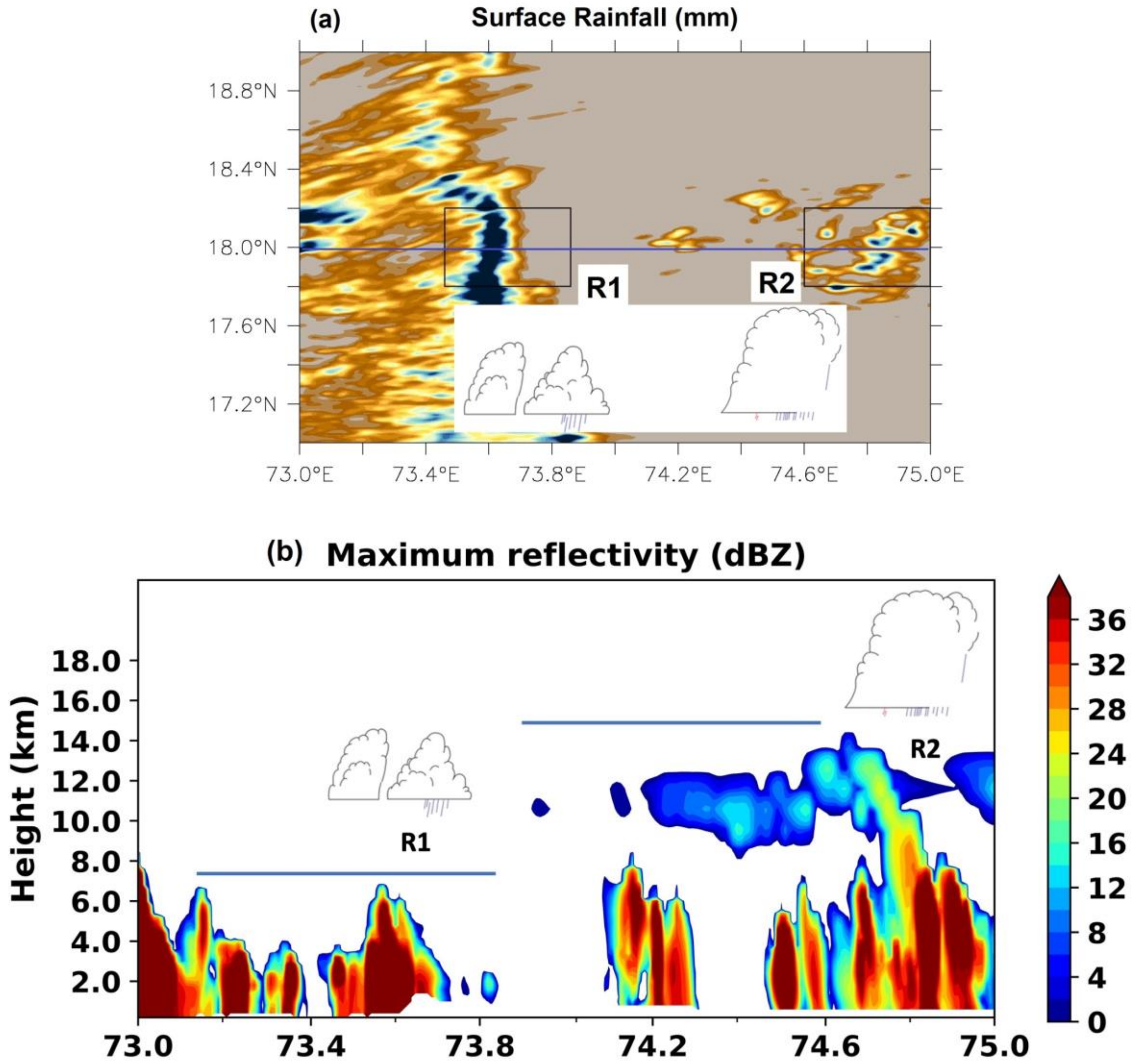
(a)
Surface Rainfall (mm)
18.8°N
18.4°N
18.0°N
17.6°N
17.2°N
73.0°E
73.4°E
73.8°E
74.2°E
74.6°E
75.0°E
R1
R2
(b)
Maximum reflectivity (dBZ)
Height (km)
18.0
16.0
14.0
12.0
10.0
8.0
6.0
4.0
2.0
73.0
73.4
73.8
74.2
74.6
75.0
R1
R2
36
32
28
24
20
16
12
8
4
0

Figure 6

Figure 7.

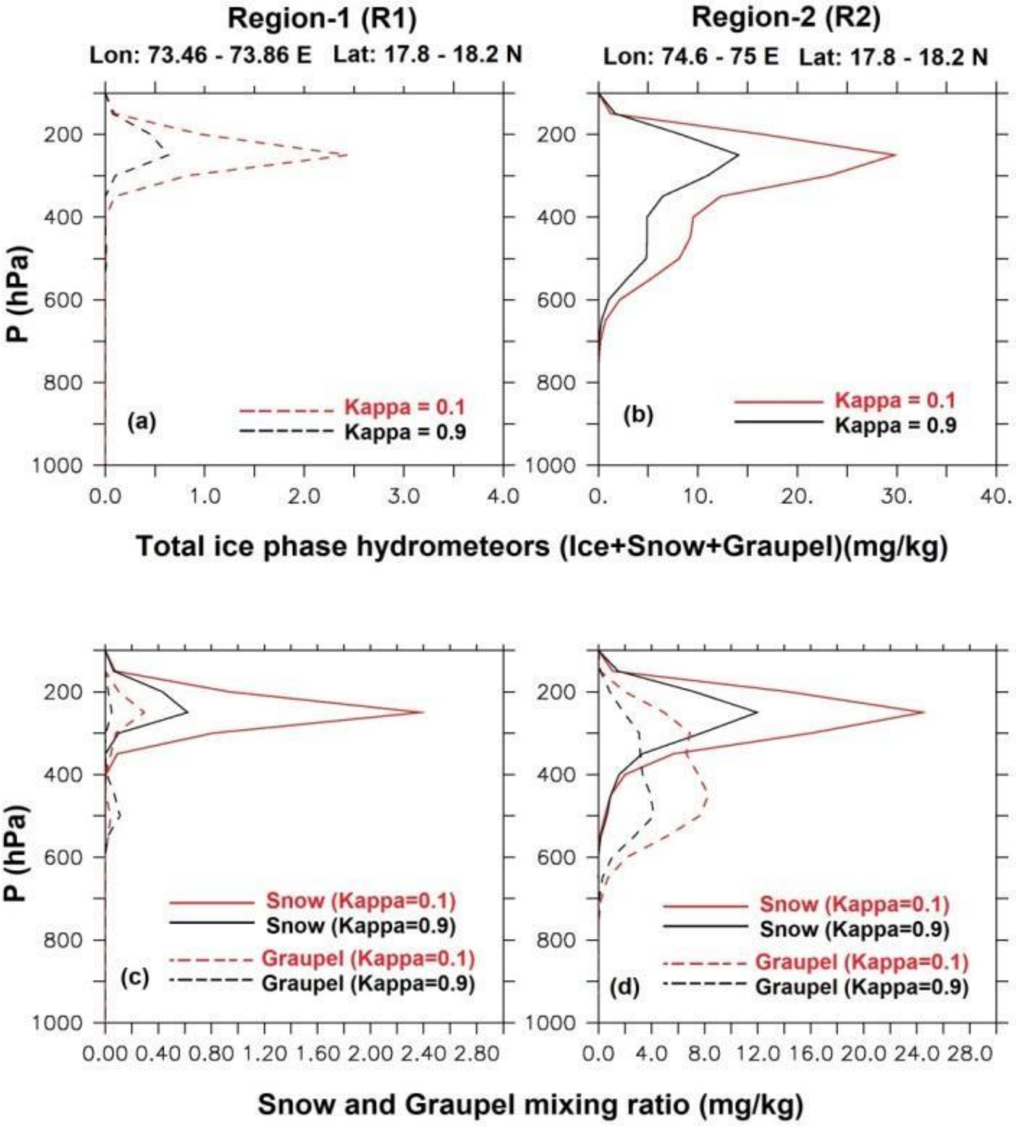

Region-1 (R1)
Lon: 73.46 - 73.86 E Lat: 17.8 - 18.2 N
Region-2 (R2)
Lon: 74.6 - 75 E Lat: 17.8 - 18.2 N
P (hPa)
200
400
600
800
1000
(a)
Kappa = 0.1
Kappa = 0.9
0.0 1.0 2.0 3.0 4.0
(b)
Kappa = 0.1
Kappa = 0.9
0. 10. 20. 30. 40.
Total ice phase hydrometeors (Ice+Snow+Graupel)(mg/kg)
(c)
Snow (Kappa=0.1)
Snow (Kappa=0.9)
Graupel (Kappa=0.1)
Graupel (Kappa=0.9)
0.00 0.40 0.80 1.20 1.60 2.00 2.40 2.80
(d)
Snow (Kappa=0.1)
Snow (Kappa=0.9)
Graupel (Kappa=0.1)
Graupel (Kappa=0.9)
0.0 4.0 8.0 12.0 16.0 20.0 24.0 28.0
Snow and Graupel mixing ratio (mg/kg)

Figure 7:

Figure 8.

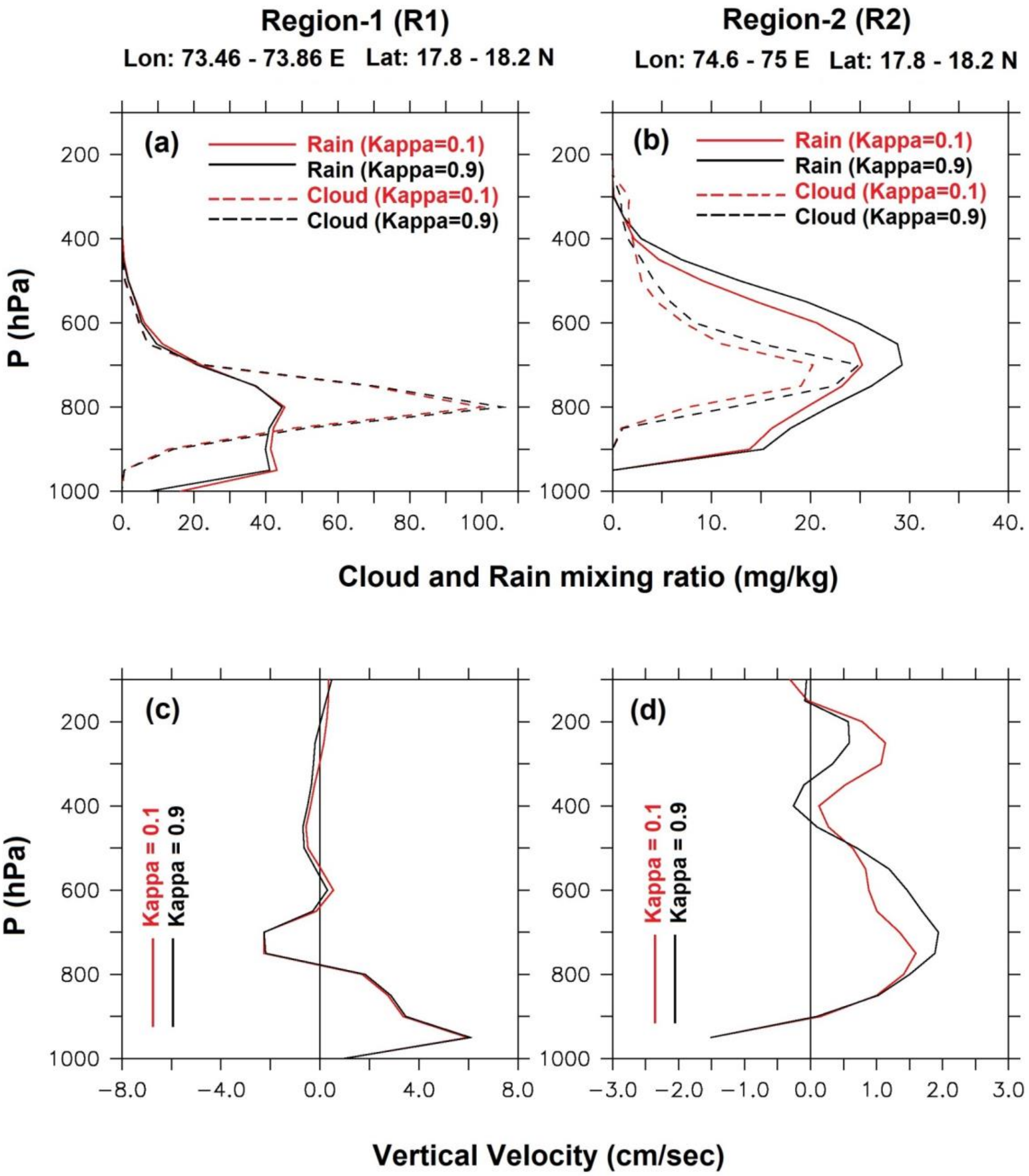

Region-1 (R1)
Lon: 73.46 - 73.86 E Lat: 17.8 - 18.2 N
Region-2 (R2)
Lon: 74.6 - 75 E Lat: 17.8 - 18.2 N
(a)
(b)
Rain (Kappa=0.1)
Rain (Kappa=0.9)
Cloud (Kappa=0.1)
Cloud (Kappa=0.9)
P (hPa)
Cloud and Rain mixing ratio (mg/kg)
(c)
(d)
Kappa = 0.1
Kappa = 0.9
Vertical Velocity (cm/sec)

Figure 8

Figure 9.

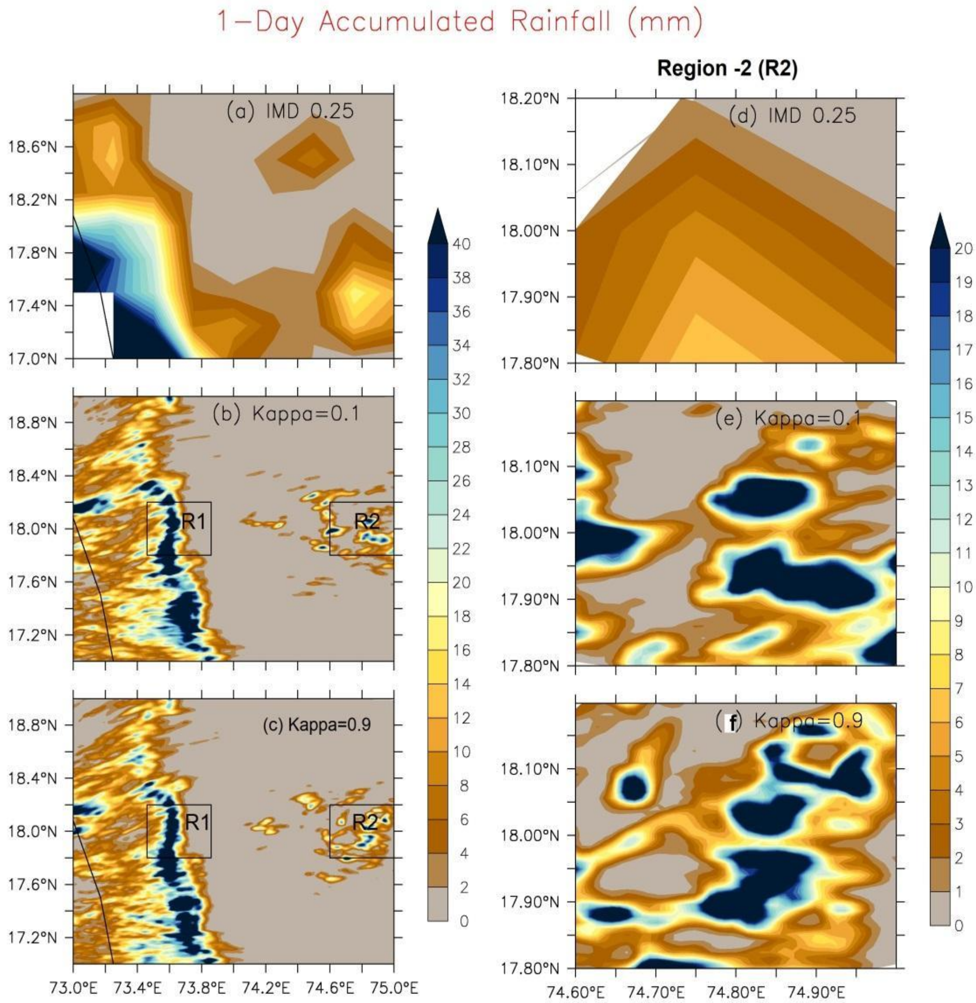

1−Day Accumulated Rainfall (mm)
Region -2 (R2)
(a) IMD 0.25
(b) Kappa=0.1
(c) Kappa=0.9
(d) IMD 0.25
(e) Kappa=0.1
(f) Kappa=0.9
R1
R2
18.6°N
18.2°N
17.8°N
17.4°N
17.0°N
18.8°N
18.4°N
18.0°N
17.6°N
17.2°N
73.0°E
73.4°E
73.8°E
74.2°E
74.6°E
75.0°E
18.20°N
18.10°N
18.00°N
17.90°N
17.80°N
74.60°E
74.70°E
74.80°E
74.90°E
40 38 36 34 32 30 28 26 24 22 20 18 16 14 12 10 8 6 4 2 0
20 19 18 17 16 15 14 13 12 11 10 9 8 7 6 5 4 3 2 1 0

Figure 9:

Figure 10.

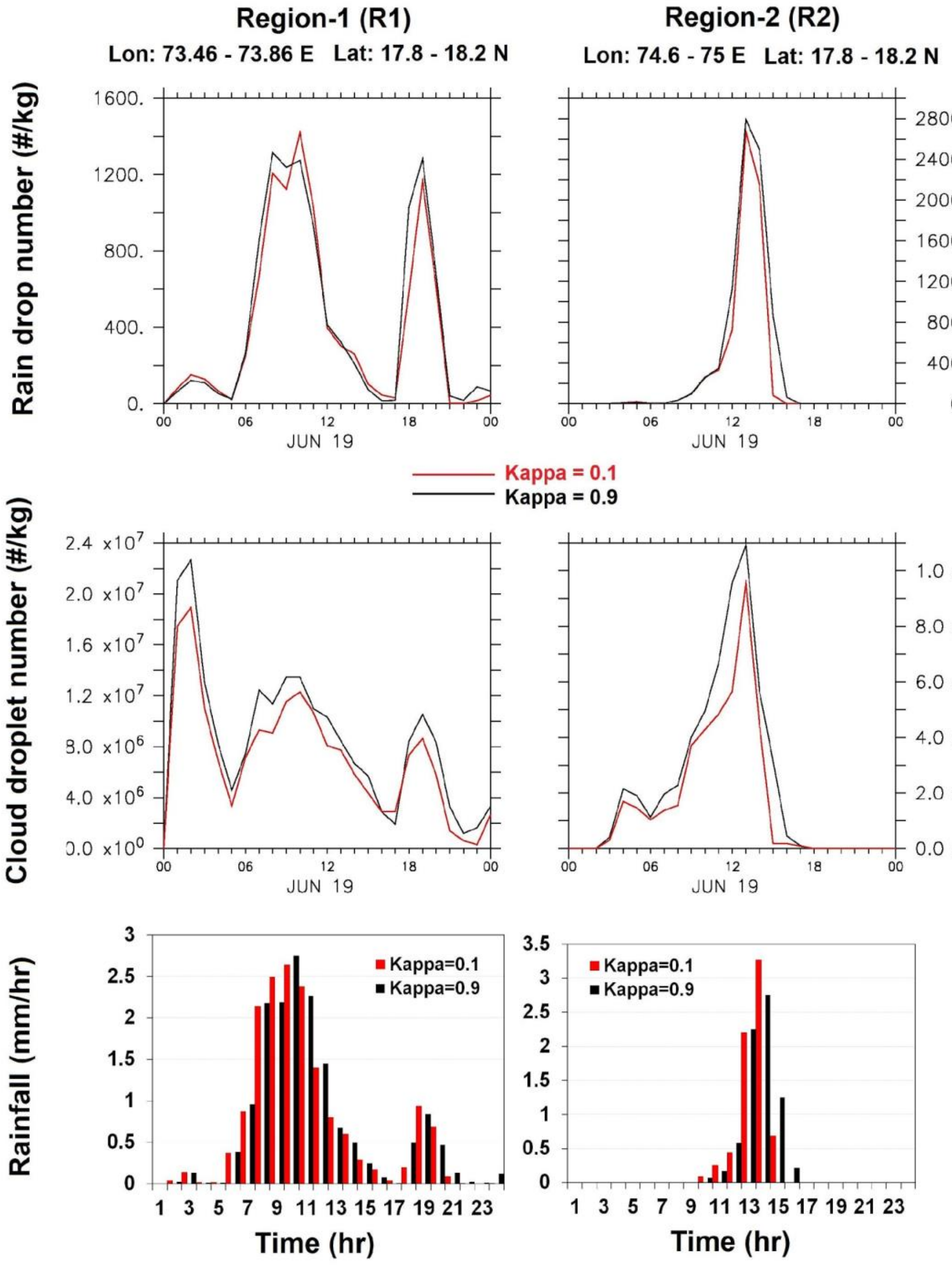
Region-1 (R1)
Lon: 73.46 - 73.86 E Lat: 17.8 - 18.2 N
Region-2 (R2)
Lon: 74.6 - 75 E Lat: 17.8 - 18.2 N
Rain drop number (#/kg)
JUN 19
Kappa = 0.1
Kappa = 0.9
Cloud droplet number (#/kg)
Rainfall (mm/hr)
Kappa=0.1
Kappa=0.9
Time (hr)

Figure 10:

Figure 11.

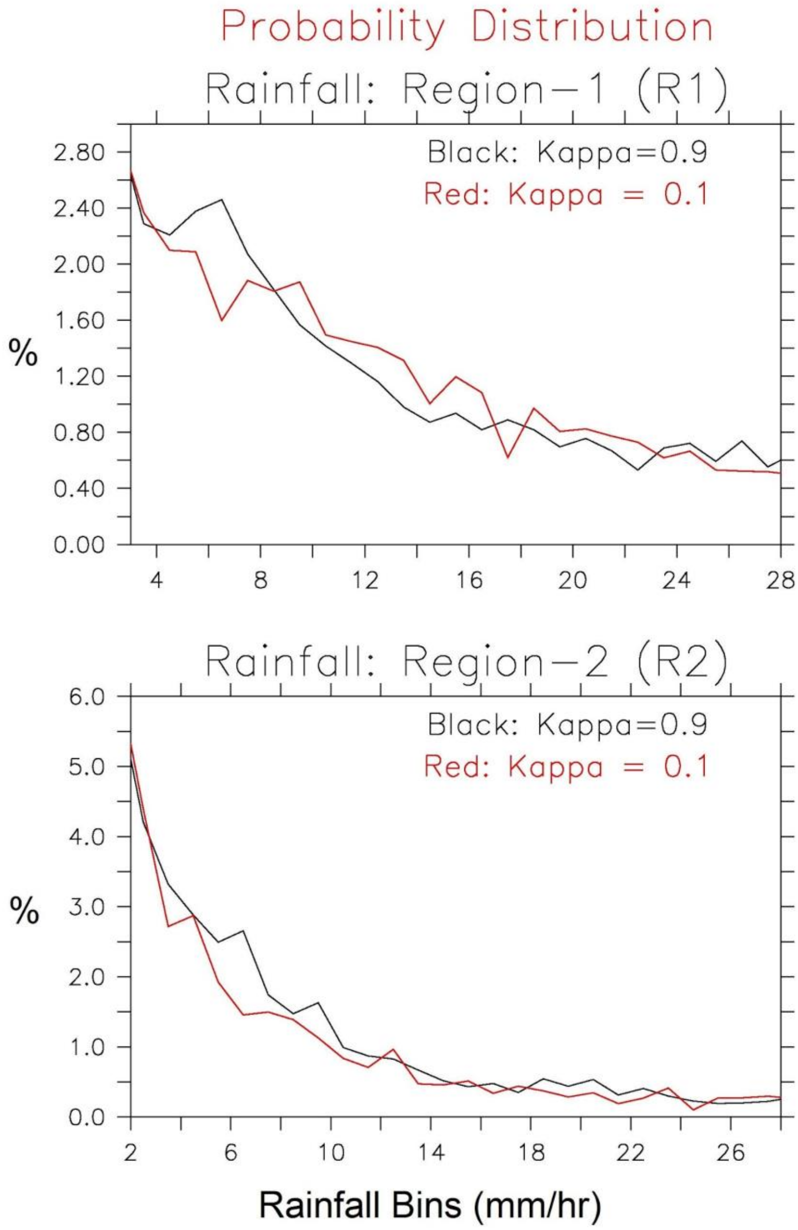
Probability Distribution
Rainfall: Region−1 (R1)
Black: Kappa=0.9
Red: Kappa = 0.1
%
2.80
2.40
2.00
1.60
1.20
0.80
0.40
0.00
4
8
12
16
20
24
28
Rainfall: Region−2 (R2)
Black: Kappa=0.9
Red: Kappa = 0.1
%
6.0
5.0
4.0
3.0
2.0
1.0
0.0
2
6
10
14
18
22
26
Rainfall Bins (mm/hr)

Figure 11:

Figure 12.

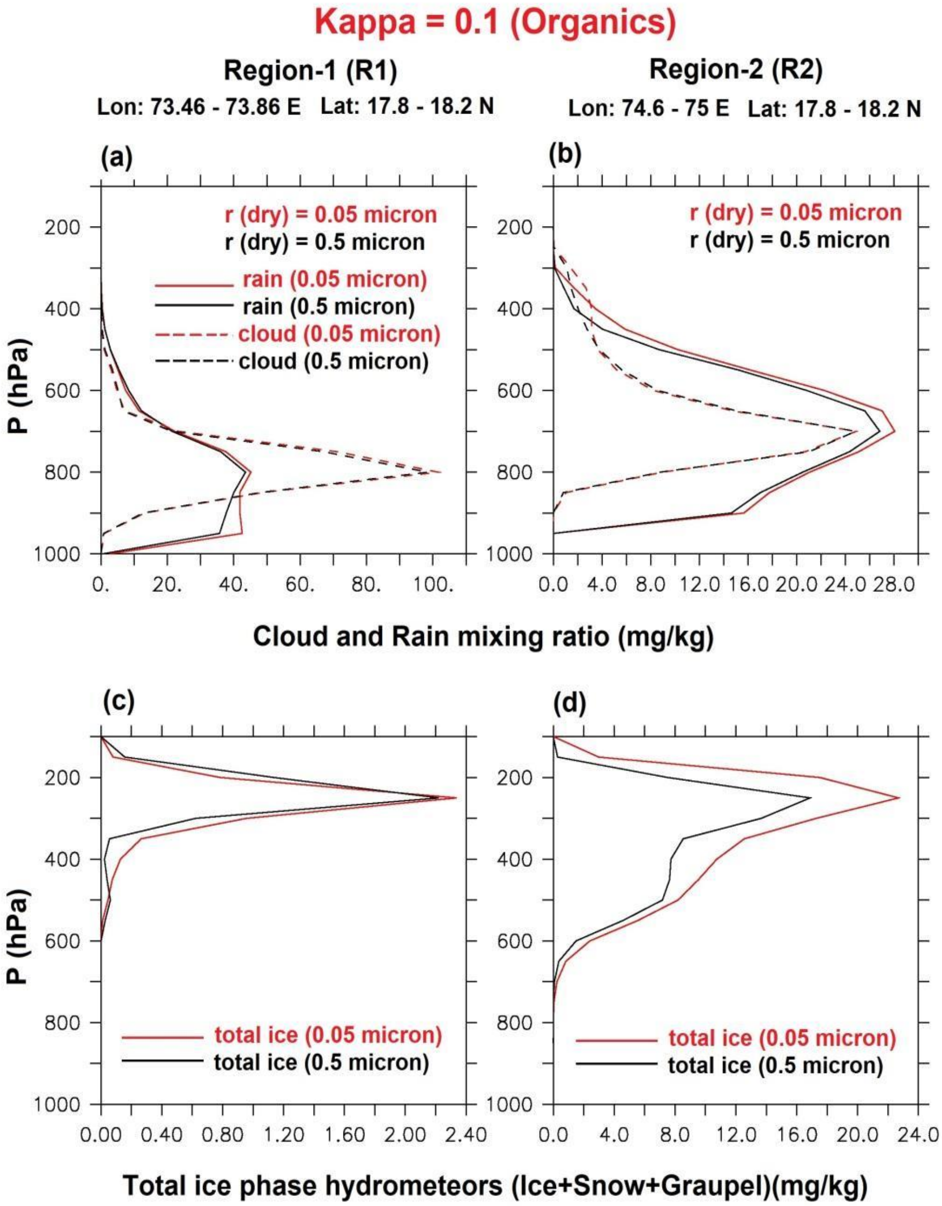

Kappa = 0.1 (Organics)
Region-1 (R1)
Lon: 73.46 - 73.86 E Lat: 17.8 - 18.2 N
Region-2 (R2)
Lon: 74.6 - 75 E Lat: 17.8 - 18.2 N
(a)
(b)
r (dry) = 0.05 micron
r (dry) = 0.5 micron
rain (0.05 micron)
rain (0.5 micron)
cloud (0.05 micron)
cloud (0.5 micron)
P (hPa)
Cloud and Rain mixing ratio (mg/kg)
(c)
(d)
total ice (0.05 micron)
total ice (0.5 micron)
Total ice phase hydrometeors (Ice+Snow+Graupel)(mg/kg)

Figure 12:

Figure 13.

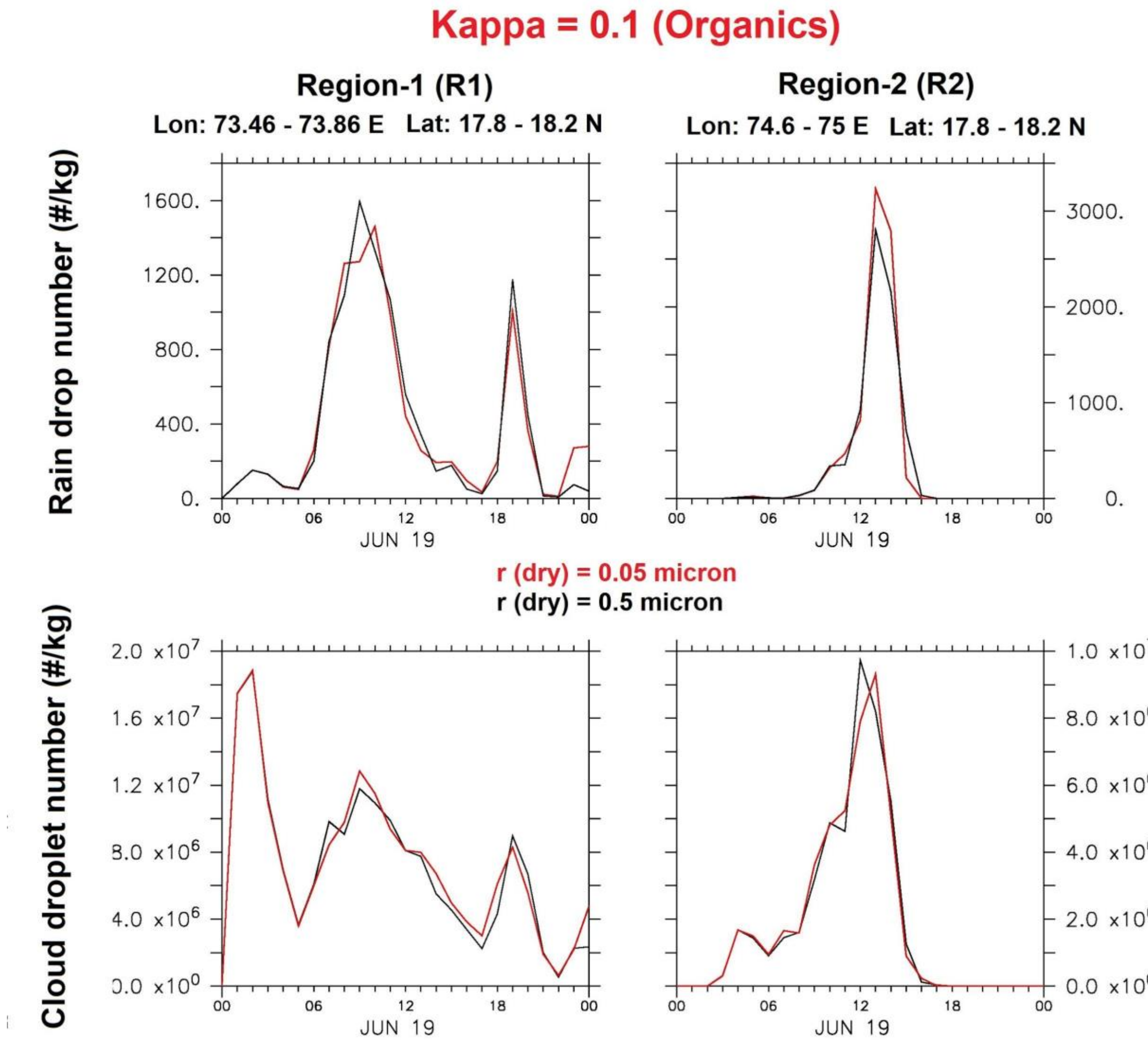

Kappa = 0.1 (Organics)
Region-1 (R1)
Lon: 73.46 - 73.86 E Lat: 17.8 - 18.2 N
Region-2 (R2)
Lon: 74.6 - 75 E Lat: 17.8 - 18.2 N
Rain drop number (#/kg)
1600.
1200.
800.
400.
0.
3000.
2000.
1000.
0.
00
06
12
18
00
JUN 19
r (dry) = 0.05 micron
r (dry) = 0.5 micron
Cloud droplet number (#/kg)
2.0 x10^7
1.6 x10^7
1.2 x10^7
8.0 x10^6
4.0 x10^6
0.0 x10^0
1.0 x10^7
8.0 x10^6
6.0 x10^6
4.0 x10^6
2.0 x10^6
0.0 x10^0

Figure 13: